

# Orbital Unsymmetrization Affects Facial Selectivities of Diels–Alder Dienophiles

Iwao Okamoto, Tomohiko Ohwada,\* and Koichi Shudo

Faculty of Pharmaceutical Sciences, University of Tokyo, 7-3-1 Hongo, Bunkyo-ku, Tokyo 113, Japan

Received November 27, 1995<sup>⊗</sup>

We investigated the Diels–Alder reactions of maleic anhydrides embedded in a dibenzobicyclo[2.2.2]octatriene motif as a nonsterically biased dienophile. Substituents on a benzene ring in these dienophiles are far from the reaction center, providing a sterically equivalent  $\pi$ -face. Instead substituents can unsymmetrize the dienophilic  $\pi$  face through  $\pi^*$  (anhydride)– $\pi^*$  (aromatic) orbital interactions. Electron-withdrawing substituents affect the facial bias and relative rates of these cycloadditions. The preference of the cycloadditions is opposite in direction to those observed in nucleophilic additions of 2-substituted-9,10-dihydro-9,10-ethanoanthracen-11-ones (dibenzobicyclo[2.2.2]octadienones) and in electrophilic additions of 2-substituted 9,10-dihydro-9,10-ethenoanthracenes (dibenzobicyclo[2.2.2]octatrienes), though all of them have related dibenzobicyclic systems.

## Introduction

Facial selectivities in Diels–Alder reactions have been intensively investigated.<sup>1</sup> There have been many experimental and theoretical studies on the behavior of facially perturbed dienes. Facial biases of dienes have been accounted for in terms of steric,<sup>1</sup> hyperconjugative,<sup>2</sup> electrostatic,<sup>3</sup> torsional,<sup>4</sup> or orbital effects.<sup>5,6</sup> In most cases, steric effect controls selectivity, but in some cases the reactions are considered to be free from steric bias,<sup>7,8</sup> and the selectivity has been explained in terms of other factors. In particular the validity of the Cieplak postulate,<sup>2</sup> i.e., hyperconjugative stabilization of an incipient

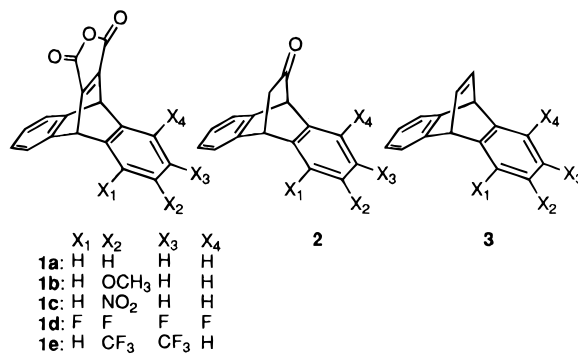


Figure 1.

bond at the transition states, is the subject of lively debate.<sup>8b,9</sup> Only a few systematic experiments have been carried out to characterize facially perturbed dienophiles. Edman and Simmons synthesized bicyclo[2.2.1]hepta-2,5-diene-2,3-dicarboxylic anhydride as a facially perturbed dienophile and observed its *exo*-selectivity in Diels–Alder reactions.<sup>10</sup> Mehta *et al.* reported a systematic investigation of the reactions of norborneno- and norbornanobenzoquinones.<sup>11</sup> Both examples concern a norbornadiene skeleton and its vinylogous  $\pi$  systems as dienophiles. We are interested in  $\pi$ -facial nonequivalence of a dienophile arising from a remote substituent, so we investigated the Diels–Alder reactions of the anhydrides **1** based on a dibenzobicyclo[2.2.2]octatriene motif as nonsterically biased dienophiles (Figure 1). Substituents in the dienophiles **1b–e** are far from the reaction center, providing a sterically equivalent  $\pi$ -face. Instead, the substituents can modify the  $\pi$  face of the dienophiles through  $\pi$ –(anhydride)– $\pi$ (aromatic) orbital interactions. We will discuss herein the substituent effect on the facial bias and on the relative rates of these cycloadditions, and the origin of these biases are postulated on the basis of orbital interactions. The preference of the cycloadditions is opposite in direction to the biases observed in nucleophilic

<sup>⊗</sup> Abstract published in *Advance ACS Abstracts*, April 1, 1996.

(1) (a) Trost, B. M.; Fleming, I., Eds.; Paquette, L. A., volume Ed. *Comprehensive Organic Synthesis*; Pergamon Press: Oxford, U. K., 1991; Vol. 5, Chapter 4. (b) Mikami, K.; Motoyama, Y.; Terada, M. *J. Am. Chem. Soc.* **1994**, *116*, 2812–2820. (c) Ishihara, K.; Yamamoto, H. *J. Am. Chem. Soc.* **1994**, *116*, 1561–1562. (d) Corey, E. J.; Sarshar, S.; Lee, D.-H. *J. Am. Chem. Soc.* **1994**, *116*, 12089–12090.

(2) Cieplak, A. S. *J. Am. Chem. Soc.* **1981**, *103*, 4540–4552. For a review: Li, H.; le Noble, W. J. *Recl. Trav. Chim. Pays-Bas* **1992**, *115*, 199–210.

(3) Dipole effects: (a) Roush, W. R.; Brown, B. B. *J. Org. Chem.* **1992**, *57*, 3380–3387. (b) Fotiadu, F.; Michel, F.; Buono, G. *Tetrahedron Lett.* **1990**, *31*, 4863–4866. (c) Kahn, S. D.; Hehre, W. J. *J. Am. Chem. Soc.* **1987**, *109*, 663. (d) Paquette, L. A.; Branan, B. M.; Rogers, R. D.; Bond, A. H.; Lange, H.; Gleiter, H. *J. Am. Chem. Soc.* **1995**, *117*, 5992–6001.

(4) (a) Brown, F. K.; Houk, K. N. *Tetrahedron Lett.* **1984**, *25*, 4609–4612. (b) Brown, F. K.; Houk, K. N. *J. Am. Chem. Soc.* **1985**, *107*, 1971–1978. (c) Storer, J. W.; Raimondi, L.; Houk, K. N. *J. Am. Chem. Soc.* **1994**, *116*, 9675–9683. (d) Review: Houk, K. N.; González, J.; Li, Y. *Acc. Chem. Res.* **1995**, *28*, 81–90. Houk, K. N.; Paddon-Row, M. N.; Rondan, N. G.; Wu, Y.-D.; Brown, F. K.; Spellmeyer, D. C.; Metz, J. T.; Li, Y.; Loncharich, R. J. *Science*, **1986**, *231*, 1108–1117. Houk, K. N.; Li, Y.; Evanseck, J. P. *Angew. Chem., Int. Ed. Engl.* **1992**, *31*, 682–708. (d) Machiguchi, T.; Hasegawa, T.; Ishii, Y.; Yamabe, S.; Minato, T. *J. Am. Chem. Soc.* **1993**, *115*, 11536–11541.

(5) Inagaki, S.; Fukui, K. *Chem. Lett.* **1974**, 509–514. Inagaki, S.; Fujimoto, H.; Fukui, K. *J. Am. Chem. Soc.* **1976**, *98*, 4054–4061. Ishida, M.; Beniya, Y.; Inagaki, S.; Kato, S. *J. Am. Chem. Soc.* **1990**, *112*, 8980–8982.

(6) Gleiter, R.; Paquette, L. A. *Acc. Chem. Res.* **1983**, *16*, 328–334. Paquette, L. A.; Carr, R. V.; Böhm, M. C.; Gleiter, R. *J. Am. Chem. Soc.* **1980**, *102*, 1186–1188. Mazzocchi, P. H.; Stahly, B.; Dodd, J.; Rondan, N. G.; Domelsmith, L. N.; Rozeboom, M. D.; Caramella, P.; Houk, K. N. *J. Am. Chem. Soc.* **1980**, *102*, 6482. Böhm, M. C.; Carr, R. V. C.; Gleiter, R.; Paquette, L. A. *J. Am. Chem. Soc.* **1980**, *102*, 7218–7228. Paquette, L. A.; Bellamy, F.; Wells, G. J.; Böhm, M. C.; Gleiter, R. *J. Am. Chem. Soc.* **1981**, *103*, 7122–7133.

(7) Halterman, R. L.; McCarthy, B. A.; McEvoy, M. A. *J. Org. Chem.* **1992**, *57*, 5585.

(8) (a) Macaulay, J. B.; Fallis, A. G. *J. Am. Chem. Soc.* **1988**, *110*, 4074–4076. (b) Macaulay, J. B.; Fallis, A. G. *J. Am. Chem. Soc.* **1990**, *112*, 1136–1144.

(9) (a) Poirier, R. A.; Pye, C. C.; Xidos, J. D.; Burnell, D. J. *J. Org. Chem.* **1995**, *60*, 2328–2329. (b) Coxon, J. M.; McDonald, D. Q. *Tetrahedron Lett.* **1992**, *33*, 651.

(10) Edman, J. R.; Simmons, H. E. *J. Org. Chem.* **1968**, *33*, 3808–3816. See also Bartlett, P. D.; Blakeney, A. J.; Kimura, M.; Watson, W. H. *J. Am. Chem. Soc.* **1980**, *102*, 1383–1390.

(11) Mehta, G.; Padme, S.; Patabhi, V.; Pramanik, A.; Chandrasekhar, J. *J. Am. Chem. Soc.* **1990**, *112*, 2942–2949.

additions of 2-substituted 9,10-dihydro-9,10-ethanoanthracen-11-ones **2** (dibenzobicyclo[2.2.2]octadienones) and in electrophilic additions of 2-substituted 9,10-dihydro-9,10-ethenoanthracenes (dibenzobicyclo[2.2.2]octatrienes) **3** (Figure 1).<sup>12</sup> We will also highlight divergent orbital interactions involved in these related dibenzobicyclo systems.<sup>13</sup>

## Results

### Syntheses of Facially Perturbed Dienophiles.

The dibenzobicyclo[2.2.2]octatriene skeleton was obtained by the Diels–Alder reaction of anthracene and dimethyl acetylenedicarboxylate (for details, see Experimental Section, Figures 4 and 5). The adduct, 9,10-dihydro-9,10-ethenoanthracene-11,12-dicarboxylic acid dimethyl ester (**4a**), was nitrated with fuming nitric acid in acetic anhydride to give the 2-nitro diester **4c**. **4c** was reduced over Fe/HCl to the 2-amino compound, and diazotization, hydrolysis, and methylation with dimethyl sulfate gave the 2-methoxy dicarboxylic acid. 1,2,3,4-Tetrafluoro- and 2,3-bis(trifluoromethyl)-9,10-dihydro-9,10-ethenoanthracene-11,12-dicarboxylic acid dimethyl esters were obtained similarly from the corresponding substituted anthracenes (1,2,3,4-tetrafluoroanthracene and 2,3-bis(trifluoromethyl)anthracene). 1,2,3,4-Tetrafluoroanthracene was prepared according to Cantrell's method.<sup>14</sup> 2,3-Bis(trifluoromethyl)anthracene was synthesized from 2,3-bis(trifluoromethyl)-9,10-dihydro-9,10-ethenoanthracene, which was obtained from the Diels–Alder reaction of 2,3-dimethylene-1,4-dihydro-1,4-ethenonaphthalene and hexafluoro-2-butyne, followed by dehydrogenation with DDQ (2,3-dichloro-5,6-dicyano-1,4-benzoquinone).<sup>15</sup> Conversion of the diester to the anhydride **1** was achieved as follows: each diester **4a–e** was hydrolyzed to the corresponding dicarboxylic acid with aqueous sodium hydroxide in methanol, and the diacid was subjected to dehydroxylation in acetic anhydride to give the corresponding anhydride, substituted 9,10-dihydro-9,10-ethenoanthracene-11,12-dicarboxylic anhydride (**1a–e**).

We investigated the Diels–Alder reactions of the anhydrides **1a–e** with two acyclic dienes, 1,3-butadiene and 2,3-dimethyl-1,3-butadiene, and with two cyclic dienes, cyclopentadiene and 1,3-cyclohexadiene. Stereogenic isomer ratios were determined from signal integration values in the <sup>1</sup>H-NMR, and the structures were confirmed by proton NOE detection.<sup>16</sup> The results of the reactions are summarized in Tables 1 and 2.

### Diels–Alder Reactions with Open-Chain Dienes.

The cycloaddition reactions of the anhydrides **1a–e** with acyclic dienes (1,3-butadiene and 2,3-dimethyl-1,3-butadiene) were conducted at 23 °C in dichloromethane as a cosolvent. Two adducts (*anti*- and *syn*-adducts) (**5/6** and **7/8**) were formed in these reactions (Figure 2 and Table 1).<sup>16,17</sup> Both of the dienes exhibited a similar substituent

**Table 1.**  $\pi$ -Facial Selectivities in Cycloadditions of Anhydride **1** with Open-Chain Dienes<sup>a</sup>

dienophile	substituent	diene <sup>b,c</sup>	temp (°C)	yield (%)	facial selectivity (ratio)	
					anti	syn
<b>1a</b>	H	BD	23	98	50	50
<b>1b</b>	2-OMe	BD	23	94	49	51
<b>1c</b>	2-NO <sub>2</sub>	BD	23	87	69	31
<b>1d</b>	1,2,3,4-tetraF	BD	23	85	64	36
<b>1e</b>	2,3-bisCF <sub>3</sub>	BD	23	96	75	25
<b>1a</b>	H	DMBD	23	100	50	50
<b>1b</b>	2-OMe	DMBD	23	98	47	53
<b>1c</b>	2-NO <sub>2</sub>	DMBD	23	95	67	33
<b>1d</b>	1,2,3,4-tetraF	DMBD	23	100	63	37
<b>1e</b>	2,3-bisCF <sub>3</sub>	DMBD	23	96	76	24

<sup>a</sup> With a solvent of methylene chloride. The reaction time is 15 h. <sup>b</sup> The reactions are carried out in a sealed bottle in the case of BD. <sup>c</sup> BD = 1,3-butadiene, DMBD = 2,3-dimethyl-1,3-butadiene.

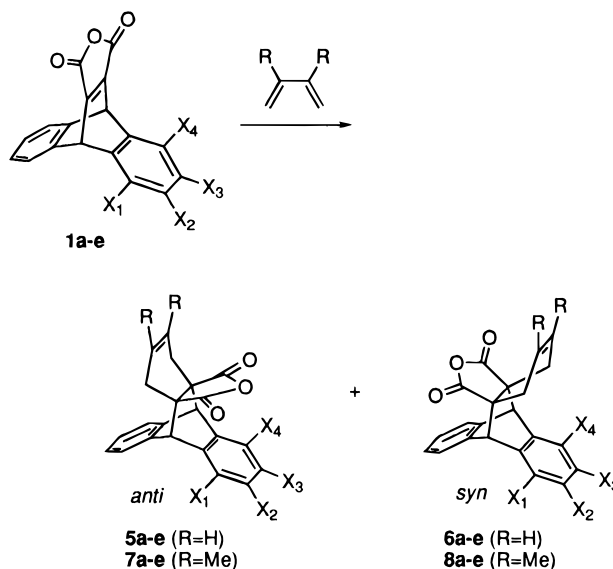


**Figure 2.**

effect: while the electron-donating methoxy-substituted dienophile **1b** showed no facial selectivity in the cycloaddition, the nitro-substituted **1c** did exhibit facial selectivity, i.e., the *anti*-addition is favored over *syn*-addition. In order to evaluate the perturbing effect of an electron-withdrawing substituent, we prepared 1,2,3,4-tetrafluoro- (**1d**) and 2,3-bis(trifluoromethyl)-substituted anhydrides (**1e**). Both substrates (**1d** and **1e**) also favored *anti*-addition over *syn*-addition: the tetrafluoro compound **1d** exhibited a similar bias (64:36) to the nitro compound, and the bis(trifluoromethyl) compound **1e** exhibited a bias as large as 75:25.

We also carried out these reactions at 80 °C using toluene in place of dichloromethane as a solvent (data shown in supporting information). A similar *anti*-preference of the cycloadditions was observed in the cases of **1c**, **1d** and **1e**, with electron-withdrawing substituents, although the magnitude of the selectivity decreased to some extent in the cases of **1c** and **1e**. Even when a mixture of the isolated *anti*-adduct **7c** of 2,3-dimethyl-1,3-butadiene and 2,3-dimethyl-1,3-butadiene in toluene was subjected to heating at 80 °C for 15 h, no isomerization was observed, and **7c** was recovered unchanged. Therefore, the product distribution was determined kinetically.<sup>18</sup>

**Diels–Alder Reactions with Cyclic Dienes. Cyclopentadiene.** We carried out Diels–Alder reactions

(12) Haga, N.; Ohwada, T.; Okamoto I.; Shudo, K. *Chem. Pharm. Bull.* **1992**, *40*, 3349–3351. Ohwada, T.; Okamoto, I.; Haga, N.; Shudo, K. *J. Org. Chem.* **1994**, *59*, 3975–3984.

(13) A part of this work was presented at the 210th American Chemical Society National Meeting, 1995, August 20–24, Chicago, Abstract ORGN 298.

(14) Cantrell, G. L.; Filler, R. *J. Fluorine Chem.* **1985**, *29*, 417

(15) Butler, D. N.; Snow, R. A. *Can. J. Chem.* **1972**, *50*, 795

(16) The structures of some of the products (**6c** and **11c**) were confirmed by X-ray crystallographic analysis.

(17) It has been found that the addition of an acyclic diene such as 1,3-butadiene and maleic anhydride leads to the product arising from the *endo* transition state. Stephenson, L. M.; Smoth, D. E.; Current, S. P. *J. Org. Chem.* **1982**, *47*, 4170.

Table 2.  $\pi$ -Facial Selectivities in Cycloadditions of Anhydride **1** with Cyclic Dienes<sup>a,b</sup>

dienophile	diene <sup>c</sup>	temp (°C)	yield (%)	facial selectivity						
				<i>anti-endo</i> , %	<i>anti-exo</i> , %	<i>syn-endo</i> , %	<i>syn-exo</i> , %	<i>endo anti:syn</i>	<i>exo anti:syn</i>	
<b>1a</b>	H	CPD	23	63	32	18	32	18	50:50	50:50
<b>1b</b>	2-OMe	CPD	23	56	34	17	33	16	50:50	51:49
<b>1c</b>	2-NO <sub>2</sub>	CPD	23	74	41	26	18	15	70:30	63:37
<b>1d</b>	1,2,3,4-tetraF	CPD	23	79	34	25	17	25	67:33	49:51
<b>1e</b>	2,3-bisCF <sub>3</sub>	CPD	23	88	44	28	13	15	77:23	65:35
<b>1a</b>	H	CHD	100	58	6	44	6	44	50:50	50:50
<b>1b</b>	2-OMe	CHD	100	61	5	46	5	44	50:50	51:49
<b>1c</b>	2-NO <sub>2</sub>	CHD	100	55	6	55	4	35	60:40	62:38
<b>1d</b>	1,2,3,4-tetraF	CHD	100	57	3	50	3	44	50:50	54:46
<b>1e</b>	2,3-bisCF <sub>3</sub>	CHD	100	50	5	48	4	43	56:44	53:47

<sup>a</sup> In the case of CPD, the reactions were carried out at 23 °C for 15 h with cosolvent of CH<sub>2</sub>Cl<sub>2</sub>. <sup>b</sup> The reaction with CHD were carried out in a sealed bottle at 100 °C without solvent. <sup>c</sup> CPD = cyclopentadiene, CHD = 1,3-cyclohexadiene.

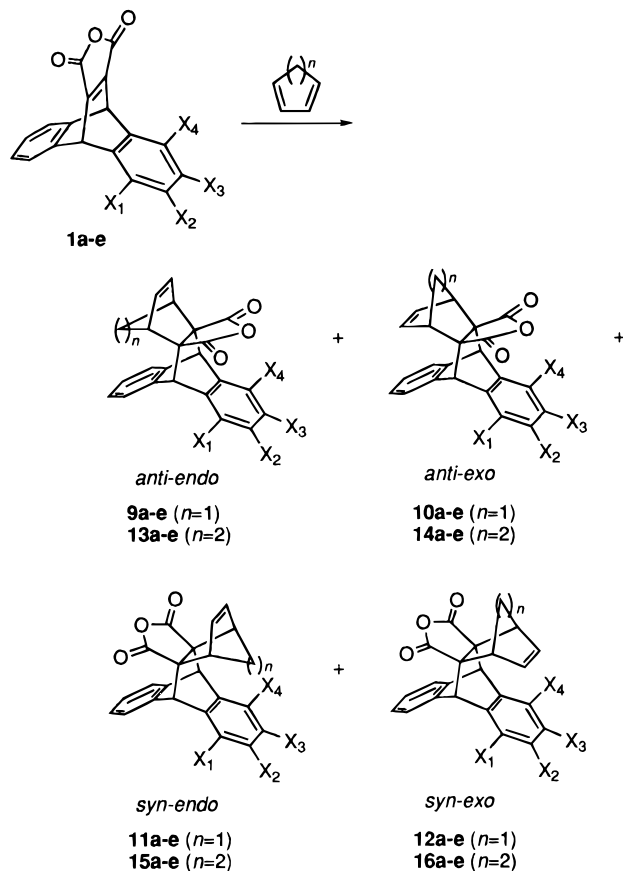


Figure 3.

of the anhydride **1** with the cyclic diene (cyclopentadiene) at 23 °C (Table 2) in dichloromethane as a solvent. The four possible adducts **9–12** (*anti-endo*, *anti-exo*, *syn-endo*, and *syn-exo*-adducts) were formed in these reactions (Figure 3). The *exo*-adduct of **1a** with cyclopentadiene (**10a** = **12a**) did not change into any other stereoisomer (**9a** = **11a**) even on heating at 80 °C for 15 h in the presence of cyclopentadiene in toluene, indicating that the distributions of products are also kinetically controlled.<sup>18</sup> Cycloadditions with cyclopentadiene exhib-

(18) If the retro-Diels–Alder reaction from the adduct **10a** to **1a** and cyclopentadiene takes place, a mixture of the *endo*- (**9a**) and *exo*-adducts (**10a**) would be formed when the isolated adduct **10a** was subjected to heating in the presence of cyclopentadiene. Furthermore, it is more likely that another type of retro-Diels–Alder reaction of **10a** leading to anthracene and bicyclo[2.2.1]hepta-2,5-diene-2,3-dicarboxylic anhydride would proceed and provide the *exo*-product (**10a**) predominantly through these fragments (see ref 10). However, these are not the experimental facts.

ited a similar substituent effect to that in the cases of the reactions with the open-chain dienes (1,3-butadiene and 2,3-dimethyl-1,3-butadiene), i.e., the methoxy-substituted derivative **1b** reacted with cyclopentadiene without facial discrimination (*anti/syn* = 51:49), although **1b** showed an *endo*-preference (*endo/exo* = 2:1) on both the *anti*- and *syn*-sides. A similar *endo/exo* ratio was found in the case of the parent substrate **1**. In the reactions of the substrates **1c–e** bearing electron-withdrawing groups, *anti*-addition is favored over *syn*-addition in both the *endo*- and *exo*-adducts (except the *endo*-adducts of **1d**). The *anti/syn* ratios increased from the tetrafluoro (**1d**) to the nitro (**1c**) and the bis(trifluoromethyl) case (**1e**); the ratios of **1e** were 77:23 (in the *endo*-adducts) and 65:35 (in the *exo*-adducts). Apparently the *anti/syn* ratios in the *endo*-adducts are larger than those in the *exo*-adducts. A close scrutiny of the results indicated that substrates **1c–e** favored *endo*-additions over *exo*-addition in the *anti*-adducts, and the *endo/exo* ratios are within the range of 1.4–1.6, quite close to the values obtained in the cases of unbiased **1a** (1.8) and **1b** (2.0). Thus, the *endo* preference observed in the *anti*-adducts seems inherent in the 9,10-dihydro-9,10-ethenoanthracene motif. On the other hand, in the *syn*-adducts of **1c–e** the *endo/exo* ratios are divergent (0.68–1.2): the *endo/exo* preference was upset in the cases of **1d** and **1e**.

When the reactions were carried out at 80 °C in toluene, the essential *anti* preference in the *endo*-adducts was conserved in the substrates **1c–e**. However the *anti/syn* selectivity is lower than those found at 23 °C. There is also a remarkable increase of *syn*-addition in the *exo*-addition of **1d** and **1e** (data shown in supporting information), resulting in loss of the *anti* preference.

**Cyclohexadiene.** We also examined the reactions of **1a–e** with 1,3-cyclohexadiene. 1,3-Cyclohexadiene is known to be much less reactive than cyclopentadiene,<sup>19</sup> and the reaction did not take place even at 80 °C in toluene; vigorous conditions were required (100 °C, neat) to give the adducts **13–16** (Table 2 and Figure 3). Substrates **1c–e** also showed *anti*-preference for the cycloadditions, but with much reduced selectivity as compared with the reaction of cyclopentadiene, probably owing to the high reaction temperature. Although maleic anhydride itself reacted with a diene exclusively in an *endo*-fashion, all the substrates **1a–e** reacted with 1,3-cyclohexadiene predominantly in an *exo*-fashion (*exo/endo* = 7.3–10.8). The steric repulsion of the methylene protons of 1,3-cyclohexadiene and the aromatic moiety may override the usual *endo* selectivity.<sup>20</sup>

(19) Rucker, C.; Lang, D.; Sauer, J.; Friege, H.; Sustmann, R. *Chem. Ber.* **1980**, *113*, 1663.

**Table 3. Relative Ratios of the Second-Order Rate Constants in Diels–Alder Reactions with 2,3-Dimethyl-1,3-butadiene**

dienophile	substituent	anti	syn	anti+syn
<b>1a</b>	H	1.00	1.00	2.00
<b>1b</b>	2-OMe	1.08	1.08	2.16
<b>1c</b>	2-NO <sub>2</sub>	2.40	1.18	3.58
<b>1d</b>	1,2,3,4-tetraF	4.86	2.98	7.84
<b>1e</b>	2,3-bisCF <sub>3</sub>	3.72	1.18	4.90

**Relative Rates of the Diels–Alder Reaction with 2,3-Dimethyl-1,3-butadiene.** In order to understand more quantitatively the nature of the substituent effect, we measured the relative rates of cycloaddition of **1b–e** in comparison with that of the parent **1a** as a reference. A solution of an equimolar mixture of one of the substituted dienophiles **1b–e** and **1a** in CD<sub>2</sub>Cl<sub>2</sub> was treated with a 2-fold molar excess of 2,3-dimethyl-1,3-butadiene, and the reaction was monitored in terms of disappearance of the proton signals of the substrates by the <sup>1</sup>H NMR spectroscopy. The relative values of the second-order rate constants at 23 °C are summarized in Table 3, wherein the reaction rate of **1a** on either side (*anti* or *syn*) is represented as 1.00 as a standard value.<sup>21</sup> The methoxy substituent has practically no effect on the reaction rate. However it is apparent that electron-withdrawing substituents (**1c**, **1d**, and **1e**) accelerate the *anti*-addition significantly, whereas in *syn*-addition the acceleration is not as large; the rate is comparable to that of the reference compound **1a**. In the reactions of the tetrafluoro-substituted dienophile **1d**, we found significant rate acceleration on both sides, while the *anti*-side addition is still substantially favored.

**Computed Transition Structures of Diels–Alder Reactions of 1.** Because structural and energetic differences in the transition structure (TS) can rationalize the observed biases,<sup>4</sup> we carried out computational evaluation of the TS of the cycloadditions of **1a**, **1c**, **1d**, and **1e** with 1,3-butadiene and cyclopentadiene, using the RHF/PM3 method<sup>22</sup> and *ab initio* minimal basis sets (RHF/STO-3G)<sup>23,24</sup> for **1a** and **1d**. *C<sub>s</sub>* symmetry was imposed except in the cases of **1c** and **1e**, which have transition structures of *C<sub>1</sub>* symmetry.<sup>25ab</sup> The transition structures obtained here are characterized by a single negative frequency which corresponds to the cycloaddition.<sup>25</sup> The lengths of the incipient bonds in the transition structures are essentially constant, within the range of 2.25 Å [2.27 Å] (PM3 and [STO-3G]) (in the reactions with 1,3-butadiene) to 2.26 Å [2.29 Å] (PM3 and [STO-3G]) (in

the reactions with cyclopentadiene) (Chart 1).<sup>4</sup> Thus the geometry of the reaction center is conserved, independent of the dienophiles and dienes. Although we could not find significant structural difference in the transition structures on the *syn* and *anti* sides among the dienophiles, it is worthwhile to compare the TS with those of the simple combination of maleic anhydride and 1,3-butadiene, and maleic anhydride and cyclopentadiene (Chart 2). The striking geometrical feature found in the dibenzobicyclo[2.2.2]octane systems (**1**) is the greatly enhanced bending of the anhydride plane (angle  $\alpha$ ) as compared with the simple cases. The degree of bending is similar in magnitude in both the *endo* and *exo* modes. This bending is due to the upward shift of the trajectory of cycloadditions,<sup>26</sup> indicated by less obtuse angles (angle  $\beta$ ), probably owing to the steric and electronic interactions of the diene with the aromatic rings of the dienophile. This modification of the trajectory retards the reaction, judging from the longer incipient bond, the lesser amounts of electron shifts (Chart 2) and the higher activation barrier (data shown in supporting information) in comparison with those of maleic anhydride.<sup>27</sup>

We calculated the PM3-based activation energy ( $\Delta E^\ddagger$ ) and the differences of potential energy between the products and the reactants ( $\Delta E$ ), in terms of the heat of formation, as well as those on the basis of the *ab initio* basis sets including HF/6-31G\* single point calculations on the STO-3G optimized geometries. The calculated differences in activation energy ( $\Delta\Delta E^\ddagger$ ) among the four possible reaction trajectories (*anti-endo*-, *anti-exo*-, *syn-endo*-, and *syn-exo*-additions) did not correspond to the experimental results as anticipated from the small values of the experimental energy differences (0.4–0.6 kcal/mol).

## Discussion

We can evidently assign the Diels–Alder reactions of **1** as normal electron-demand reactions, which involve a primary orbital interaction between the LUMO of **1** and the HOMO of the diene.<sup>28,29</sup> This conclusion is supported by the calculated electron shift from the diene to the dienophile in the TS (Chart 2). It is also supported by the fact that 9,10-dihydro-9,10-ethenoanthracene (**3**) itself and the 11,12-bis(methoxycarbonyl) derivatives **4** did not undergo Diels–Alder reactions with hydrocarbon dienes (1,3-butadiene or cyclopentadiene). The electron-withdrawing functionality of the anhydride in **1** is prerequisite for the reaction.

Here we present a rather intuitive analysis of the orbital interactions leading to unsymmetrization of the dienophilic  $\pi$  face.

**Orbital Unsymmetrization of Anhydride Dienophile.  $\pi$  Fragment Orbitals and Combinations.** In order to analyze the unsymmetrization of the  $\pi$ -face of the anhydride **1** within the framework of perturbation theory,<sup>28c,30</sup> we disconnect the dienophile molecule into

(20) Houk, K. N.; Luskus, L. J. *J. Am. Chem. Soc.* **1971**, *93*, 4606–4607. See also Kobuke, Y.; Fueno, T.; Furukawa, J. *J. Am. Chem. Soc.* **1970**, *92*, 6548–6553.

(21) Because a mixture of the two dienophiles is treated with a single diene, the relative value of the rate constants is independent of the concentration of the diene.

(22) MOPAC (version 6.0): Stewart, J. J. P. QCPE program No. 455. Revised as MOPAC (version 6.01 and 6.02) by Prof. Tsuneo Hirano, Ochanomizu University, for HITAC version. *JCPE Newsletter* **1991**, *2*, 26. The eigenvector following method was used to optimize the TS, and cartesian coordinates were used for **1c** and **1e**.

(23) Hehre, W. J.; Radom, L.; Schleyer, P. V. R.; Pople, J. A. *Ab Initio Molecular Orbital Theory*; Wiley and Sons, Inc.: New York, 1986.

(24) Gaussian 92: M. J. Frisch, G. W. Trucks, M. Head-Gordon, P. M. W. Gill, M. W. Wong, J. B. Foresman, B. G. Johnson, H. B. Schlegel, M. A. Robb, E. S. Replogle, R. Gomperts, J. L. Andres, K. Raghavachari, J. S. Binkley, C. Gonzalez, R. L. Martin, D. J. Fox, D. J. Defrees, J. Baker, J. J. P. Stewart, and J. A. Pople, Gaussian, Inc., Pittsburgh, PA, 1992.

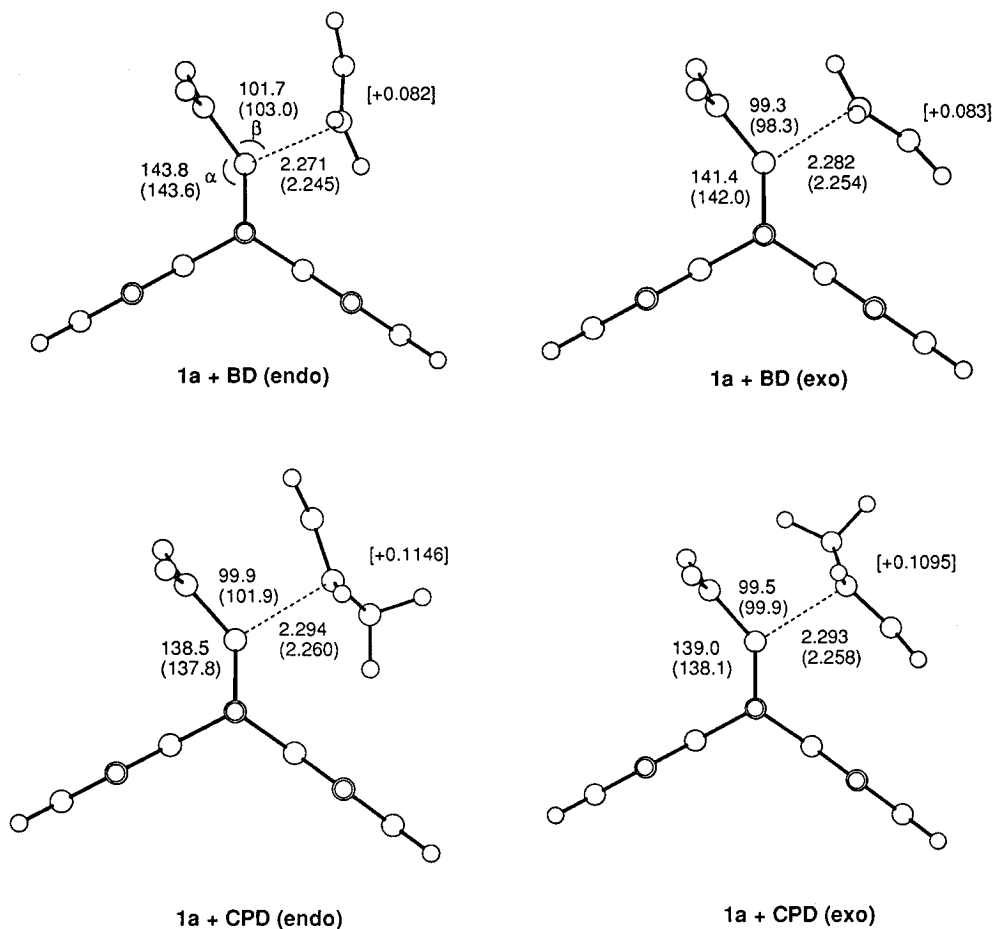
(25) (a) McIver, J. W., Jr.; Stanton, R. E. *J. Am. Chem. Soc.* **1972**, *94*, 8618–8620. (b) McIver, J. W., Jr. *Acc. Chem. Soc.* **1974**, *7*, 71–77. (c) McIver, J. W.; Komornicki, A. *J. Am. Chem. Soc.* **1972**, *94*, 2625. (d) Komornicki, A.; Ishida, K.; Morokuma, K.; Ditchfield, R.; Conrad, M. *Chem. Phys. Lett.* **1977**, *45*, 595. See also ref 40.

(26) Bürgi, H. B.; Dunitz, J. D.; Scheffter, E. *J. Am. Chem. Soc.* **1973**, *95*, 5065–5067. Bürgi, H. B.; Lehn, J. M.; Wipff, G. *J. Am. Chem. Soc.* **1974**, *96*, 1956. Bürgi, H. B.; Dunitz, J. D.; Lehn, J. M.; Wipff, G. *Tetrahedron* **1974**, *30*, 1563–1572. Bürgi, H. B. *Angew. Chem., Int. Ed.* **1975**, *14*, 460–473.

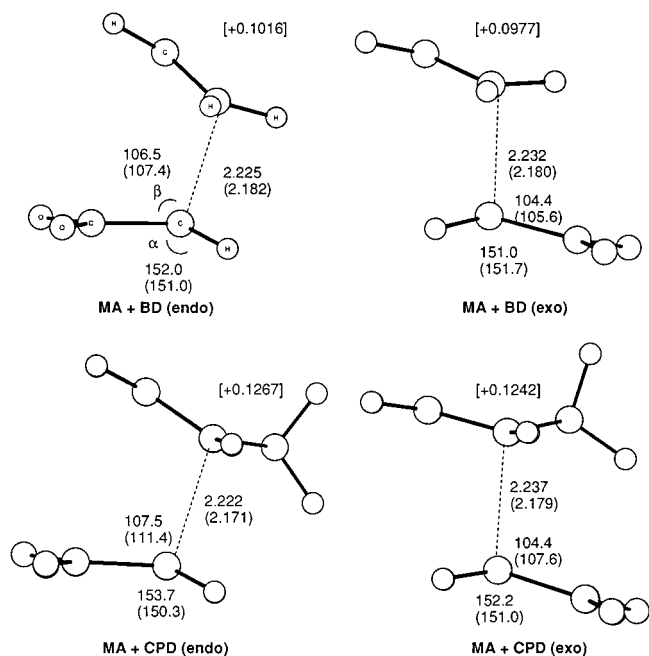
(27) Sato, M.; Murakami, M.; Sunami, S.; Kaneko, C.; Furuya, T.; Kurihara, H. *J. Am. Chem. Soc.* **1995**, *117*, 4279–4287.

(28) (a) Fujimoto, H.; Inagaki, S.; Fukui, K. *J. Am. Chem. Soc.* **1976**, *98*, 2670–2671. (b) Fukui, K. *Science*, **1982**, *218*, 747–754, and references cited therein. (c) Fukui, K. *Theory and Orientation and Stereoselection*; Springer-Verlag: Berlin, Heidelberg, 1975.

(29) Fleming, I. *Frontier Orbitals and Organic Chemical Reactions*; John Wiley & Son: New York, 1976.

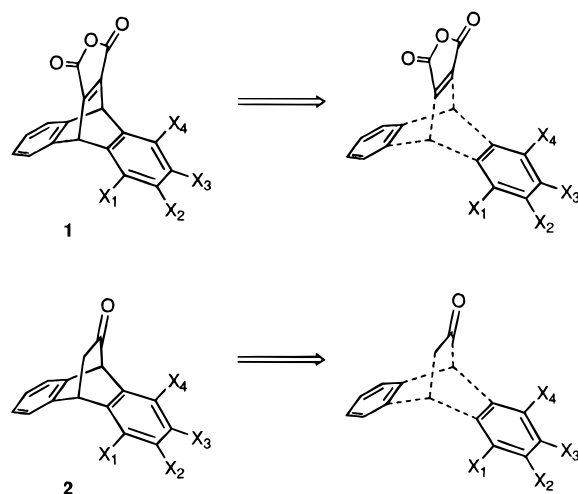
**Chart 1. STO-3G Optimized Transition Structures of Cycloadditions<sup>a</sup>**

<sup>a</sup> Selected geometrical parameters are shown, together with those obtained in PM3 optimizations (in parentheses). The electron shift (STO-3G) from the diene to the dienophile is shown in brackets. Positive values mean electron donation from the diene to the dienophile.

**Chart 2. STO-3G Optimized Transition Structures of MA and BD, and MA and CPD<sup>a</sup>**

<sup>a</sup> See captions to Chart 1.

three parts, i.e., the maleic anhydride as the reaction center and two aromatic parts constituting the substituted convex dihydroanthracene (Scheme 1).<sup>12</sup> The LUMO

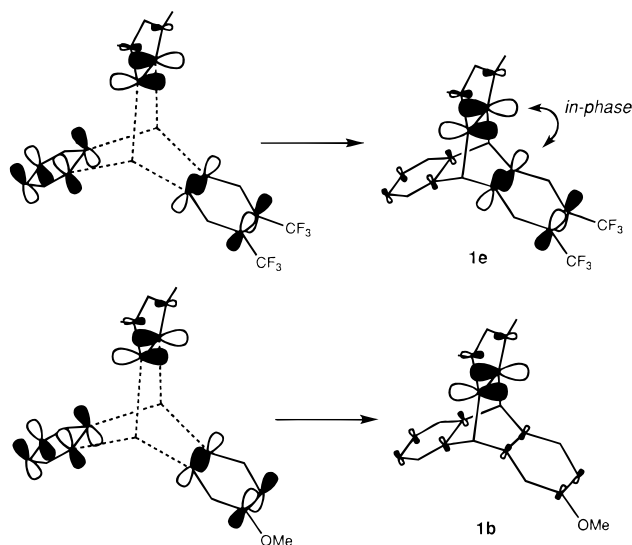
**Scheme 1. Disconnection and Recombination of the LUMO of the Dienophile 1 and the Ketone 2**

of the whole dienophile molecule **1** can be approximated as being made up by in-phase combination of the LUMOs of these three components through  $\pi$ - $\pi$  interactions.<sup>12,31</sup>

(30) (a) Libit, L.; Hoffmann, R. *J. Am. Chem. Soc.* **1974**, *96*, 1370–1383. (b) Albright, T. A.; Burdett, J. K.; Whangbo, M.-H. *Orbital Interactions in Chemistry*; John Wiley & Sons, Inc.: New York, 1985. (c) Rauk, A. *Orbital Interaction Theory of Organic Chemistry*; John Wiley & Sons, Inc.: New York, 1994.

(31) Klein, J. *Tetrahedron Lett.* **1973**, 4307–4310. Klein, J. *Tetrahedron* **1974**, *30*, 3349–3353.

**Scheme 2. Unsymmetrized and Symmetric Dienophilic  $\pi^*$  Orbital**



Because the  $\pi^*$  orbital of the anhydride moiety, i.e., maleic anhydride, is lower-lying in energy than those of the aromatic fragments, the anhydride moiety contributes predominantly to the LUMO of the whole **1**. Because an electron-withdrawing substituent lowers the energy of the (NX)LUMO ( $\pi^*$  orbitals) of the substituted benzene,<sup>29</sup> the energy gap from the  $\pi^*$  orbital (LUMO) of maleic anhydride is decreased. Therefore the  $\pi^*$  orbital of the maleic anhydride moiety interacts preferentially with the  $\pi^*$  orbital of the benzene substituted with the electron-withdrawing group (B1 orbital in the case of the nitro group, and A2 orbital in the cases of the tetrafluoro and bis(trifluoromethyl) groups) in an in-phase manner. Thus, the coefficients of the resultant LUMO of the whole dienophile molecule are localized on the substituted benzene as well as the anhydride moiety, not on the unsubstituted benzene (Scheme 2).<sup>32</sup> We have confirmed this type of orbital interaction by drawing orbital pictures.

**Symmetry-Disfavored Orbital Interactions.** Orbital mixing is accompanied with perturbation of the orbital energy level.<sup>28–30</sup> Owing to the in-phase combination of the anhydride  $\pi^*$  orbital with the aromatic  $\pi^*$  orbital, the energy level of the resultant LUMO of the dienophile is lowered. As the energy gap between the LUMO of the dienophile and the HOMO of the dienes is decreased, the reaction is activated.<sup>33</sup> Thus, the observed rate acceleration of the cycloadditions of **1c–e** on the *anti* side is a reasonable outcome. However, the reaction on the *syn* side seemed to be unaffected or much less favored except in the case of the tetrafluoro substituent (*vide supra*). In addition to this observation, the *endo/exo* ratios (in the cases of cyclic dienes) varied more significantly on the side of the substituent than on the opposite

side, depending on the substituent. Therefore the  $\pi$  lobes of the maleic anhydride moiety received a significant perturbing effect on the side of the substituent. This conclusion coincides with the localized distribution of the LUMO coefficients of the dienophile.

It is known that a remote electron-withdrawing substituent (such as a nitro group) also perturbs the  $\pi$  face of the related  $\pi$  systems of 9,10-dihydro-9,10-ethanoanthracen-11-ones **2** (in the reduction of the carbonyl group) and 9,10-dihydro-9,10-ethenoanthracenes **3** (in the epoxidation and dihydroxylation of the olefin group).<sup>12</sup> The observed bias is a *syn*-preference, opposite to that in the Diels–Alder reaction. According to the frontier orbital theory, the reaction of the ketone involves orbital interactions between the LUMO of the molecule and the HOMO of the hydride.<sup>28,29</sup> The LUMO of the ketone **2** is assumed to be built up by in-phase combinations of the fragments wherein the aromatic fragments are common, as in the case of the dienophile **1** (Scheme 1).<sup>12</sup>

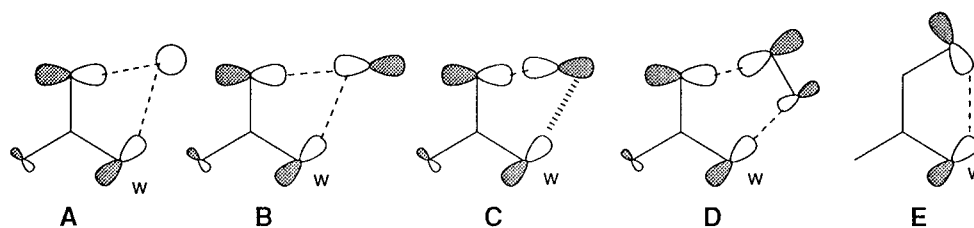
It is also known that isodicyclopentadiene and norbornene exhibit divergent stereoselectivity to cycloadditions and additions, which is attributed to different steric and torsional effects<sup>4</sup> or an orbital tilting effect.<sup>5,6</sup> However, these factors seemed not to be important in the present system (*vide ante*). Therefore the divergent substituent effect depends on the type of reaction, in particular, on the reagent: the hydride anion can be regarded as an s-orbital reagent, and a diene as a p-orbital reagent. Thus, we postulate that the retardation at the *syn* face stems from unfavorable orbital interaction developing along the *syn* attack trajectory: as the diene approaches the anhydride moiety (either in *endo* or *exo* fashion), initially favorable in-phase interaction of the  $\pi$  lobes at C<sub>1</sub> and C<sub>4</sub> of the diene with the  $\pi^*$  lobes of the aromatic moiety of the dienophile occurs (Scheme 3, **B**), in addition to the primary in-phase orbital interaction of the anhydride with the diene, as in the case of the attack of the hydride anion on the ketone (Scheme 3, **A**).<sup>34</sup> However, this interaction will start to be counteracted by the emergence of out-of-phase interaction of the  $\pi$ -back lobe of the diene with the aromatic  $\pi^*$  orbital of the dienophile. This situation can be regarded as a type of noninteraction, as depicted in Scheme 3 (**C**) with some simplification.<sup>35,36</sup> It is known that primary HOMO (diene)–LUMO (dienophile) interaction does not provide stabilization at the incipient stage of the Diels–Alder cycloaddition because of narrowing of the inter-frontier level separation (orbital narrowing); i.e., raising the energy level (i.e., destabilization) of the HOMO and lowering the energy level of the LUMO.<sup>38</sup> However, the driving force of the cycloadditions depends significantly on the stabilization of the in-phase-combined  $\pi$  orbitals (of HOMO (diene)–LUMO (dienophile)), generating stable  $\sigma$  bonds, i.e. the conjugated  $\pi$  bonds of butadiene are transformed into two  $\sigma$  bonds in the product.<sup>39</sup> This

(32) Orbital pictures based on the PM3 method confirmed the orbital interactions discussed here in the combined molecules, intermediate convex dihydroanthracenes, and the whole anhydrides **1**. The LUMOs of unsubstituted dihydroanthracene or hydroxydihydroanthracene have orbital distributions precisely or approximately symmetric in amplitude and phase with respect to the maleic anhydride plane, respectively. Therefore the LUMO of the aromatic moiety does not interact with the LUMO of the maleic anhydride owing to the symmetry disagreement in **1a** and **1b**.

(33) Sustmann, R.; Trill, H. *Angew. Chem., Int. Ed. Engl.* **1972**, *11*, 838–840. Sustmann, R.; Schubert, R. *Angew. Chem., Int. Ed. Engl.* **1972**, *11*, 840–840. See also Ishida, M.; Kakita, S.; Inagaki, S. *Chem. Lett.* **1995**, 469–470.

(34) In the HOMO ( $\chi_2$ ) of the dienes (1,3-butadiene, 2,3-dimethyl-1,3-butadiene, cyclopentadiene, and 1,3-cyclohexadiene) the coefficients of the reacting carbon atoms (C<sub>1</sub> and C<sub>2</sub>) predominate over those of the C<sub>2</sub> and C<sub>3</sub> carbon atoms. In the cycloaddition process, mixing-in of the NXLUMO ( $\chi_4^*$ ) of the diene is encouraged by orbital symmetry, resulting in localization of the coefficients at the reacting C<sub>1</sub> and C<sub>2</sub> carbons (and finally conversion into two stable  $\sigma$  orbitals).

(35) This orbital picture (Scheme 3 (**C**)) may oversimplify the orbital rehybridization and orbital energy changes resulting from geometrical distortion of addends. There is a difference in the trajectory of addition between the *endo* and *exo* modes. However, they can be represented in terms of second-order mixing of the s and p orbitals into the  $\pi$  (and  $\pi^*$ ) orbitals of the initial reactants. Therefore the primary orbital interaction, depicted in Scheme 3 (**C**), should still be maintained even in the vicinity of the transition state.

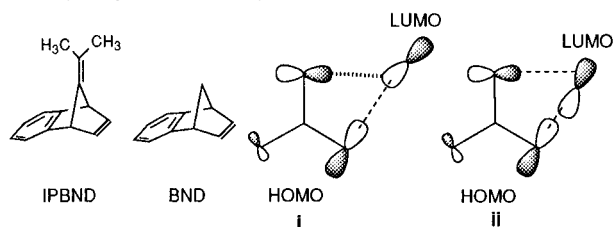
Scheme 3. Modes of Orbital Interactions (Side View)<sup>a</sup>

<sup>a</sup> w = an electron-withdrawing group.

stabilization emerges at a relatively late stage of the reaction coordinates, although an early transition state would be consistent with the exothermicity of the cycloaddition.<sup>40</sup>

To emphasize the perturbation of the internuclear region owing to the in-phase orbital interaction in the dienophile **1**, the buildup of a bonding electron is equivalent to diffusion of the electron into each bonding region along the bond axis, as depicted in Scheme 4a.<sup>41</sup> The late-developing antibonding interaction of the  $\pi^*$ -back lobe of the diene will be enhanced by such an internuclear diffused region (Scheme 4b). Therefore, this late-developing orbital phase disagreement may modify the

(36) Large rate acceleration was encountered in the reverse-electron-demand Diels–Alder cycloadditions of 7-isopropylidenebenzonorbornadiene (IPBND) as compared with benzenorbornadiene (BND) (as a dienophile) in the reaction of tropone (as an electron-deficient diene) (ref 37c). As pointed out in ref 37d, the initial orbital interaction of the HOMO of IPBND (the dienophile) and the LUMO of the diene is a noninteracting one because of the orbital symmetry disagreement (i), leading to decreased reactivity of IPBND. Thus, the observed large acceleration and high *exo*-selectivity of IPBND may also be rationalized in terms of favorable late-developing  $\pi^*$  back-lobe interaction of the diene (the LUMO) with the HOMO of IPBND (ii), rather than the sterically congested secondary orbital interactions proposed in ref 37c.



(37) (a) Gleiter, R.; Ginsburg, D. *Pure Appl. Chem.* **1979**, *51*, 1301–1315. (b) Hoffmann, R.; Woodward, R. B. *J. Am. Chem. Soc.* **1965**, *87*, 4388–4389. (c) Pfaendler, H. R.; Tanida, H.; Haselbach, E. *Helv. Chim. Acta*, **1974**, *57*, 383–394. (d) Haselbach, E.; Rossi, M. *Helv. Chim. Acta*, **1976**, *59*, 278–290. (e) Böhm, M.; Gleiter, R. *Tetrahedron* **1980**, *36*, 3209–3217. (f) Apeloig, Y.; Matzner, E. *J. Am. Chem. Soc.* **1995**, *117*, 5375–5376.

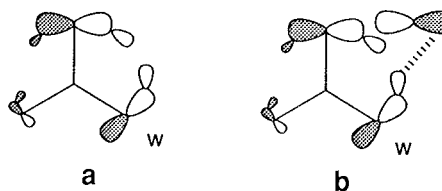
(38) Fukui, K.; Fujimoto, H. *Bull. Chem. Soc. Jpn.* **1968**, *41*, 1989–1997. Fukui, K.; Fujimoto, H. *Bull. Chem. Soc. Jpn.* **1969**, *42*, 3399–3409.

(39) Woodward, R. B.; Hoffmann, R. *The Conservation of Orbital Symmetry*; Verlag Chemie: Weinheim, 1970.

(40) Frontier orbital energy changes for the synchronous Diels–Alder reaction affording cyclohexene are discussed in Townshend, R. E.; Ramunni, G.; Segal, G.; Hehre, W. J.; Salem, L. *J. Am. Chem. Soc.* **1976**, *98*, 2190–2198. Bach, R. D.; McDouall, J. J. W.; Schegel, H. B.; Wolber, G. J. *J. Org. Chem.* **1989**, *54*, 2931–2935. On the other hand, calculational studies demonstrated that borohydride addition to formaldehyde proceeds through a single-step mechanism with a nonsynchronous four-center TS with a productlike geometry, indicating an early bond-formation interaction as depicted in Scheme 3A. Eisenstein O.; Schlegel, H. B.; Kayser, M. M. *J. Org. Chem.* **1982**, *47*, 2886–2891. Bonaccorsi, R.; Palla, P.; Tomasi, J. *J. Mol. Struct. (THEOCHEM)* **1982**, *87*, 181–196.

(41) In order to emphasize electron density distribution of the internuclear region in addition to the phase relation of the interacting orbitals, we adopted the diagram depicted in Scheme 4a. The removal of a bonding electron from the internuclear region can be regarded as diffusion of the electron of each fragment into each antibonding region along the internuclear axis; the buildup of a bonding electron is equivalent to diffusion of the electron into each bonding region along the bond axis. Ohwada, T. *J. Am. Chem. Soc.* **1992**, *114*, 8818–8827.

Scheme 4

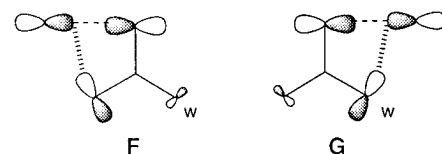


trajectory of the addition (probably causing an upward shift of the diene) on the *syn* side, leading to destabilization,<sup>26</sup> although a significant change in trajectories could not be recognized in the present calculations.

In the *exo* mode, the *syn* addition can also involve attractive secondary orbital interaction (Scheme 3, **D**)<sup>37</sup> (between the C<sub>2</sub> and C<sub>3</sub>  $\pi$  lobes of the diene and the aromatic  $\pi^*$  orbital of the dienophile), which will cancel the effect of the above out-of-phase interaction. This is compatible with the observed independence of the ratios of the *syn-exo* mode upon substitution. In contrast, the *anti*-side addition is favored in two respects: (1) genuine in-phase overlap of the LUMO of **1** and the HOMO of the diene leads to stabilization,<sup>42</sup> (2) the significant tilting of the anhydride moiety (toward the substituted benzene) provides an opportunity for the occupied  $\pi$  orbitals of the anhydride oxygen atoms to interact with the lower-lying aromatic  $\pi^*$  orbitals of the electron-deficient aromatic ring, which leads to stabilization (Scheme 3, **E**).<sup>43</sup>

**Contribution of Alternative Mechanism. Electrostatic Attraction.** The large rate increase on both

(42) It is shown that closed-shell repulsions and orbital energy changes dominate the incipient stage of the Diels–Alder reaction, rather than the frontier orbital stabilization (ref 41). This destabilization is attributed to the out-of-phase interaction of the  $\pi$  orbital of the olefin (the HOMO of the dienophile) and the  $\chi_1$  (the lowest occupied  $\pi$  orbital, NXHOMO) of the diene. The observed biases in the anhydride **1** seem superficially to be rationalizable in terms of the magnitude of this two-orbital, four-electron destabilization (**F**): the HOMO of the anhydride **1** is comprised of the out-of-phase combination of the  $\pi$  orbital of the olefin with those of aromatic orbitals (B1 symmetry). Because an electron-withdrawing substituent lowers the  $\pi$  orbitals of the benzene, the HOMO of the anhydrides **1c**, **1d**, and **1e** is derived by the out-of-phase combination of the  $\pi$  orbital of the unsubstituted benzene and the  $\pi$  orbital of the olefin. Therefore, the incipient interaction of the HOMO of the dienophile and the filled  $\chi_1$  orbital of the diene (1,3-butadiene, 2,3-dimethyl-1,3-butadiene, and cyclopentadiene) is symmetry-disfavored (**F**), a sort of orbital noninteraction, leading to relief of the four-electron destabilization interaction on the *anti* side of the substituent. However, this type of noninteraction (**G**) also exists on the NXHOMO of the dienophile, favoring the *syn* reaction. As pointed out by Inagaki et al. (Ishida, M.; Inagaki, S. *J. Synth. Org. Chem. Jpn.* **1994**, *52*, 649–657, and ref 30b, chapter 2) these two-orbital, four-electron destabilization effects are canceled out because the energy gap is inert to such destabilization. On the other hand, the two-electron case of the relevant orbital interaction motif was proposed in the rationalization of the *syn* preference of dibenzobicyclo[2.2.2]octatrienes **3** in electrophilic oxidative reactions (ref 12).



## Scheme 5. Orbital Rehybridization

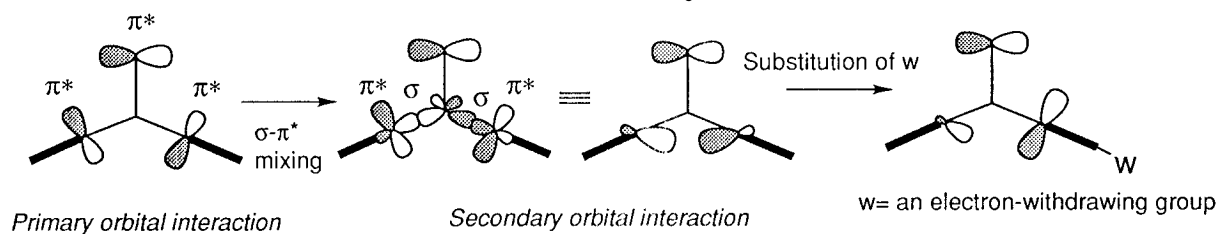
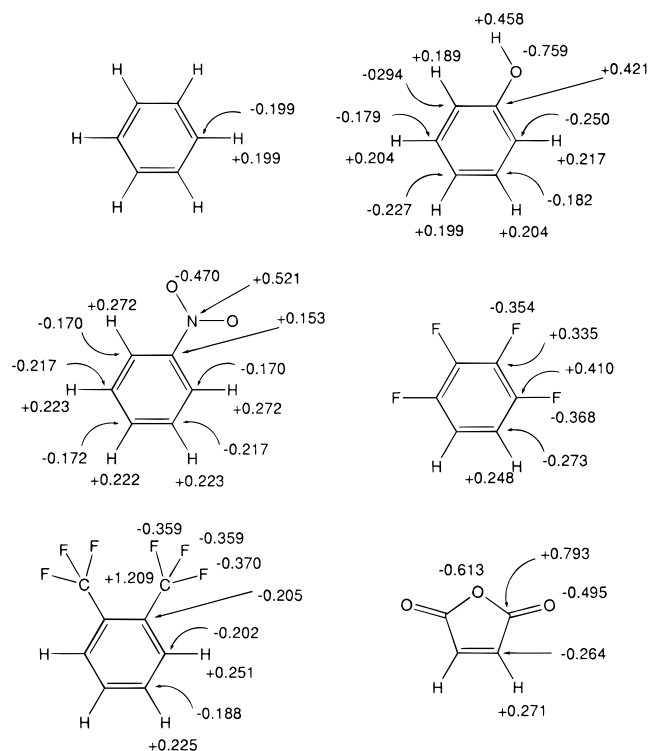


Chart 3. Mulliken Population Charges of HF/6-31G\* Optimized Geometries



sides in the tetrafluoro case is not accounted for by a simple consideration of the LUMO level. Only this substrate bears four substituents, in particular, at the C<sub>2</sub> and C<sub>5</sub> positions relatively close to the reaction center. A Mulliken population analysis<sup>44</sup> of the aromatic fragment, tetrafluorobenzene (Chart 3) on the basis of HF/6-31G\* basis sets indicates creation of positive charge at the nearest ipso positions (C<sub>2</sub> and C<sub>5</sub>) which can attract the negatively charged oxygen atoms of the anhydride moiety (in the *anti* attack) or the forming olefinic carbon atoms of the diene moiety (in the *syn* attack).<sup>45</sup> These electrostatic interactions can be operative in other cases (**1c** and **1e**), but the remote position of the positively charged region would attenuate the effect.

**Orbital Rehybridization.** Although orbital rehybridization of the  $\pi$  orbital of the reaction center through  $\sigma$ - $\pi$  mixing is important in some Diels-Alder reactions,<sup>5,6</sup> there is no significant rehybridization of the  $\pi^*$  orbital of the anhydride group in the present dienophiles. Instead, rehybridization (outward bending and mixing-

in of s orbitals) of the peripheral aromatic  $\pi^*$  orbital is detected, probably due to the antibonding mixing-in of the C-C  $\sigma$  (or sp-hybrid) orbital to the primitive (in-phase) combination of the  $\pi^*$  orbitals of the anhydride and aromatic moieties (Scheme 5).<sup>5</sup> Substitution of an electron-withdrawing group on the aromatic ring would decrease orbital tilting (i.e.,  $\sigma$ - $\pi^*$  mixing) of the aromatic  $\pi^*$  orbital, indicating a small contribution of  $\sigma$  orbital component owing to enlargement of the energy gap between the  $\sigma_{C-C}$  orbital and  $\pi_{aromatic}^*$  orbitals because of the stabilization of the  $\sigma$  orbital. This orbital picture can be approximated to a simple primary combination of  $\pi^*$  orbitals of the fragments, as depicted in Scheme 2. It might be a general case that  $\sigma$ - $\pi$  ( $\sigma$ - $\pi^*$ ) mixing at the reaction center is not significant in dienophiles such as maleic anhydride derivatives (**1**), probably because the electron-withdrawing nature of the anhydride moiety lowers the  $\sigma_{C-C}$  orbital of the relevant C-C double bond, leading to diminution of the effect of the  $\sigma$  component.

## Conclusion

We have revealed the substituent effect on the dienophilic facial selectivities of maleic anhydride embedded in the dibenzobicyclo[2.2.2]octatriene motif. The substituent effect is divergent from those observed in related ketone and olefin derivatives. These behaviors depend on the reagents, which involve different types of primary interacting orbitals, i.e. s-orbital or p-orbital reagent, and different trajectories of the addition, and in particular a different position of emergence of the HOMO-LUMO stabilization along the reaction coordinates.<sup>40</sup> The present work also provides an additional systematic example of facially perturbed dienophiles bearing a different structural motif from the previously reported norbornane system.

## Experimental Section

**General Methods.** All the melting points were measured with a Yanagimoto hot-stage melting point apparatus (MP-500) and are uncorrected. Proton NMR spectra were measured on a JEOL GX 400-MHz NMR spectrometer with TMS as an internal reference in CDCl<sub>3</sub> as the solvent. High-resolution mass spectra (HRMS) were recorded on a JEOL SX-102 instrument. Infrared spectra (IR) were recorded on a Shimadzu IR-408 instrument. High-performance liquid chromatography (HPLC) was run on a Shimadzu LC-6A system on silica gel SIL S-5 (SH-043-5, YMC, Japan) packing (20 mm × 25 cm) with the specified eluent. Flash column chromatography was performed on silica gel (Kieselgel 60, 230-400 mesh, Merck) with the specified solvent. Thin layer chromatography was performed on precoated TLC plates (Kieselgel 60, F-254, Merck). 2,3-Dimethyl-1,3-butadiene and 1,3-cyclohexadiene were commercially available (Aldrich) and were used without further purification. 1,3-Butadiene was distilled to the flask which was cooled at -78 °C. Cyclopentadiene was freshly distilled,<sup>46</sup> and the purity was checked by <sup>1</sup>H NMR. The combustion analyses were carried out in the microanalytical laboratory of this faculty.

(43) Ishida, M.; Aoyama, T.; Kato, S. *Chem. Lett.* **1989**, 663. Weinstein, S.; Lewin, A. H.; Panda, K. C. *J. Am. Chem. Soc.* **1963**, 85, 2324.

(44) Mulliken, R. S.; *J. Chem. Phys.* **1955**, 23, 1833, 1841, 2338, 2343.

(45) The electron-withdrawing tetrafluoro substituents, in particular at the C<sub>2</sub> and C<sub>5</sub> positions, can also lower the LUMO level of **1d** in a through-bond manner, which should be at least partially responsible for the rate acceleration on both sides of **1d**.



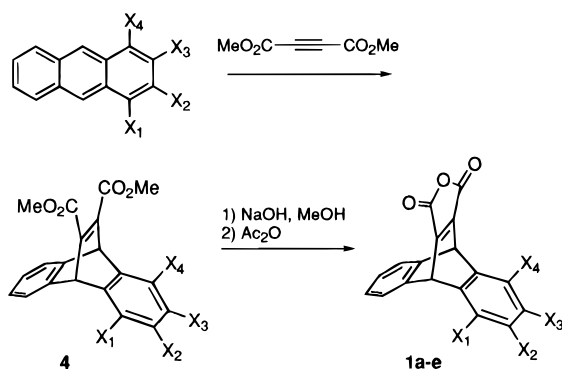


Figure 4. Preparation of the anhydrides **1a-e**.

**Preparation of Dimethyl 9,10-Dihydro-9,10-ethenoanthracene-11,12-dicarboxylate (4a).** A mixture of 10.2 g (562 mmol) of anthracene and 250 mL (2.03 mol, 3.6 equiv) of dimethyl acetylenedicarboxylate was heated at 110 °C for 22 h and then poured into cold methanol (800 mL) and washed with more 600 mL of cold methanol to give 116.0 g (64%) of **4a**. **4a**: mp 160.5–161.5 °C (colorless prisms, recrystallized from methanol).

**Hydrolysis of the Diester to 9,10-Dihydro-9,10-ethenoanthracene-11,12-dicarboxylic Acid.** To a solution of **4a** (10.02 g, 31.3 mmol, obtained as above) in methanol (120 mL) was added aqueous NaOH (2 N) (180 mL), and the mixture was heated at 60 °C for 6 h, followed by acidification with aqueous HCl (2 N). The whole mixture was extracted with ether (900 mL), and the organic phase was washed by brine, dried over MgSO<sub>4</sub>, and then evaporated to give 8.90 g (97%) of the diacid. Mp 247.5–248.5 °C (colorless needles, recrystallized from water). IR (KBr, cm<sup>-1</sup>): 3400, O–H; 1695, C=O. Anal. Calcd for C<sub>18</sub>H<sub>12</sub>O<sub>4</sub>: C, 73.97; H, 4.14. Found: C, 73.67; H, 3.93.

**9,10-Dihydro-9,10-ethenoanthracene-11,12-dicarboxylic Anhydride (1a).** **Method A.** A mixture of 2.766 g (9.46 mmol) of the diacid (obtained as above), 16.38 g (138 mmol, 7.3 equiv) of thionyl chloride, and a catalytic amount of DMF (*N,N*-dimethylformamide) was refluxed for 2 h. Remaining thionyl chloride was removed under reduced pressure to give the crude acid chloride. The resultant acid chloride was dissolved in pyridine (8 mL) and was treated with 165 mg of water (9.17 mmol, 1 equiv with respect to the acid chloride), and the mixture was allowed to stir at 18 °C for 10 min. The reaction mixture was poured into a vigorously stirred mixture of aqueous HCl (2 N, 200 mL) and 200 mL of dichloromethane. The organic layer was separated, washed with 2 N aqueous HCl, saturated aqueous sodium bicarbonate, and brine, and was dried over sodium sulfate. Evaporation of the solvent gave 1.873 g (72%) of the anhydride **1a**.

**Method B.** A mixture of the diacid (195 mg, 0.677 mmol) and 8 mL of acetic anhydride was heated at 70 °C for 5 h. Unreacted acetic anhydride was removed under reduced pressure to give the anhydride **1a** (158 mg, 85%), after washing with *n*-hexane: mp 258.0–260.0 °C (colorless prisms, recrystallized from benzene). IR (KBr, cm<sup>-1</sup>): 1840, 1765, C=O. Anal. Calcd for C<sub>18</sub>H<sub>10</sub>O<sub>3</sub>: C, 78.83; H, 3.68. Found: C, 79.13; H, 3.56.

**Nitration of Dimethyl 9,10-Dihydro-9,10-ethenoanthracene-11,12-dicarboxylate (4a).** Acetic anhydride (80 mL) was added in one portion to a weighted amount of fuming HNO<sub>3</sub> (6.1 g, 93%) at –43 °C (acetonitrile–dry ice). The mixture was stirred at –43 °C for 3 min, and then the solution of **4a** (20.0 g, 62.5 mmol) in dichloromethane (methanol-free, 100 mL) was added dropwise. After being stirred at –43 °C for 12 h, the whole mixture was added to 500 mL of ice and water and extracted with methylene chloride. The extract was washed with brine and dried over sodium sulfate. Evaporation of the solvent gave a residue (20.6 g), which was flash-

chromatographed (ethyl acetate:*n*-hexane 1:4) to give 13.1 g (57%) of dimethyl 2-nitro-9,10-dihydro-9,10-ethenoanthracene-11,12-dicarboxylate (**4c**): mp 166.5–168.0 °C (pale yellow prisms, recrystallized from methanol). Anal. Calcd for C<sub>20</sub>H<sub>15</sub>NO<sub>6</sub>: C, 65.75; H, 4.14; N, 3.83. Found: C, 65.89; H, 4.10; N, 3.87.

**2-Nitro-9,10-dihydro-9,10-ethenoanthracene-11,12-dicarboxylic Acid.** Hydrolysis of the above diester **4c** gave 2-nitro-9,10-dihydro-9,10-ethenoanthracene-11,12-dicarboxylic acid in quantitative yield. IR (KBr, cm<sup>-1</sup>): 3400, O–H; 1705, C=O; 1515, 1340, NO<sub>2</sub>.

**2-Nitro-9,10-dihydro-9,10-ethenoanthracene-11,12-dicarboxylic Anhydride (1c).** Dehydroxylation of the above diacid gave **1c** in 38% yield (method A), and 87% yield (method B), respectively. **1c**: mp 130 °C (pale brown powder, recrystallized from benzene). IR (KBr, cm<sup>-1</sup>): 1840, 1770, C=O; 1515, 1345, NO<sub>2</sub>. Anal. Calcd for C<sub>18</sub>H<sub>9</sub>NO<sub>5</sub>·<sup>1/3</sup>H<sub>2</sub>O: C, 64.79; H, 3.20; N, 4.20. Found: C, 64.63; H, 3.23; N, 4.30.

**Preparation of 2-Methoxy-9,10-dihydro-9,10-ethenoanthracene-11,12-dicarboxylic Anhydride (1b).** **(A) Reduction of Dimethyl 2-Nitro-9,10-dihydro-9,10-ethenoanthracene-11,12-dicarboxylate.** A solution of the nitro diester **4c** (5.41 g, 14.8 mmol) in 500 mL of ethanol was heated under gentle reflux in the presence of diluted aqueous HCl (2 N, 20 mL) and iron powder (20 g) with vigorous stirring. After 1 h, the cold mixture was poured into saturated aqueous sodium bicarbonate and extracted with methylene chloride. The residue was flash-chromatographed (dichloromethane) to give 4.60 g (93%) of dimethyl 2-amino-9,10-dihydro-9,10-ethenoanthracene-11,12-dicarboxylate.

**(B) Diazotization and Hydrolysis to 2-Hydroxy-9,10-dihydro-9,10-ethenoanthracene-11,12-dicarboxylic Acid.** To a solution of dimethyl 2-amino-9,10-dihydro-9,10-ethenoanthracene-11,12-dicarboxylate (4.21 g, 12.5 mmol) in acetic anhydride (40 mL) was added 11 mL of concentrated sulfuric acid slowly and followed by the addition of a solution of sodium nitrite (1.27 g, 18.5 mmol, 1.47 equiv) in water (10 mL) over 5 min at 0 °C. After being stirred for 15 min at 0 °C, urea (0.444 g, 7.39 mmol) was added in one portion. After the mixture was stirred at 0 °C for 15 min, the resultant solution of the diazonium ion was added in portions to a preheated (to gentle reflux) solution of concentrated sulfuric acid (12 mL) in 100 mL of water over 40 min. After heating for another 10 min, the mixture was extracted with methylene chloride and evaporated to give black-brown viscous oil (3.91 g). This residue was dissolved in aqueous sodium hydroxide (2 N, 100 mL), and the mixture was heated at 60 °C for 4.8 h. The cold mixture was acidified with aqueous hydrochloric acid (2 N) and then extracted with ethyl acetate, followed by evaporation to give 3.50 g (91% from the 2-amino diester) of 2-hydroxy-9,10-dihydro-9,10-ethenoanthracene-11,12-dicarboxylic acid.

**(C) Methylation to 2-Methoxy-9,10-dihydro-9,10-ethenoanthracene-11,12-dicarboxylic Acid.** The above 2-hydroxy diacid (3.17 g) was dissolved in aqueous 3 N NaOH (100 mL), and dimethyl sulfate (27 mL, 286 mmol) was added at ambient temperature. The reaction mixture was heated at 60 °C for one night. The cold mixture was acidified (pH = 1) with aqueous hydrochloric acid, and the whole was extracted with ethyl acetate. The residue was flash-chromatographed (chloroform:methanol 9:1) to give 2.69 g (81%) of 2-methoxy-9,10-dihydro-9,10-ethenoanthracene-11,12-dicarboxylic acid. IR (KBr, cm<sup>-1</sup>): 3400, O–H; 1700, C=O.

**(D) 2-Methoxy-9,10-dihydro-9,10-ethenoanthracene-11,12-dicarboxylic Anhydride (1b).** Dehydroxylation of the above diacid gave the anhydride **1b** in 79% yield (method A), and 98% yield (method B), respectively. **1b**: mp 176.0–178.0 °C (pale yellow powder, recrystallized from toluene). IR (KBr, cm<sup>-1</sup>): 1840, 1770, C=O. Anal. Calcd for C<sub>19</sub>H<sub>12</sub>O<sub>4</sub>·<sup>6/5</sup>H<sub>2</sub>O: C, 70.02; H, 4.45. Found: C, 69.98; H, 4.45.

**Dimethyl 1,2,3,4-Tetrafluoro-9,10-dihydro-9,10-ethenoanthracene-11,12-dicarboxylate (4d).** The 1,2,3,4-tetrafluoro diester **4d** was prepared by the Diels–Alder cyclization of 1,2,3,4-tetrafluoroanthracene (3.61 g, 14.42 mmol)<sup>14</sup> and 7 mL of dimethyl acetylenedicarboxylate (57 mmol, 4.0 equiv) in 88% yield (4.976 g, 12.68 mmol). **4d**: mp 112.0–113.0 °C (colorless

(46) Moffett, R. B. *Organic Syntheses*; Wiley: New York, 1963; Vol. 4, pp 238–241.

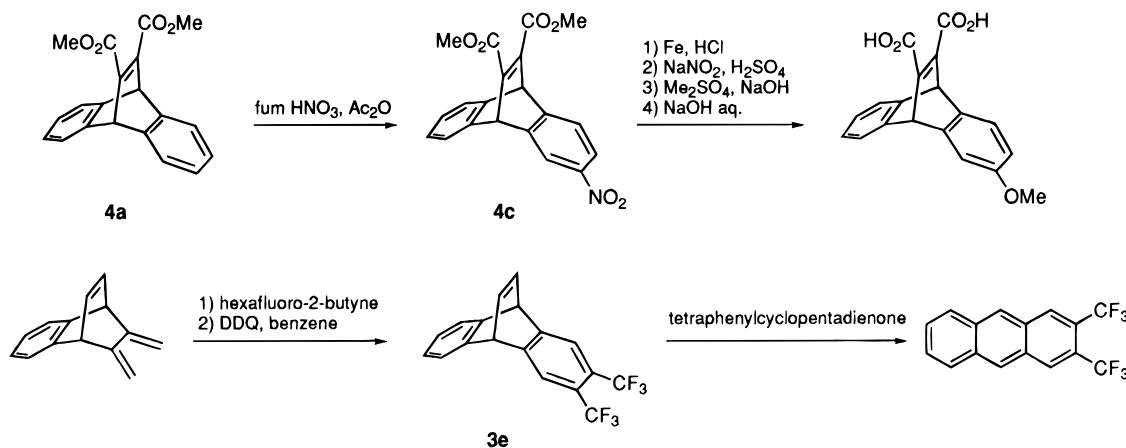


**Figure 5.** Preparation of precursors.

prisms, recrystallized from methanol). Anal. Calcd for  $C_{20}H_{12}O_4F_4$ : C, 61.23; H, 3.08. Found: C, 61.07; H, 2.79.

**1,2,3,4-Tetrafluoro-9,10-dihydro-9,10-ethenoanthracene-11,12-dicarboxylic Acid.** Hydrolysis of the above diester **4d** gave 1,2,3,4-tetrafluoro-9,10-dihydro-9,10-ethenoanthracene-11,12-dicarboxylic acid in 96% yield. Mp 253 °C dec. IR (KBr,  $cm^{-1}$ ): 3400, O—H; 1695, C=O. Anal. Calcd for  $C_{18}H_8O_4F_4 \cdot \frac{1}{3}H_2O$ : C, 58.39; H, 2.27. Found: C, 58.13; H, 2.03.

**1,2,3,4-Tetrafluoro-9,10-dihydro-9,10-ethenoanthracene-11,12-dicarboxylic Anhydride (1d).** Dehydroxylation of diacid obtained as above gave **1d** in 55% yield (method A), and 52% yield (method B). IR (KBr,  $cm^{-1}$ ): 1845, 1780, C=O. HRMS ( $M^+$ ) Calcd for  $C_{18}H_6O_3F_4$ : 346.0253. Found: 346.0271.

**Preparation of 2,3-Bis(trifluoromethyl)-9,10-dihydro-9,10-ethenoanthracene-11,12-dicarboxylic Anhydride (1e).**

**(A) 2,3-Bis(trifluoromethyl)-1,4,9,10-tetrahydro-9,10-ethenoanthracene.** A mixture of 9,10-dimethylene-1,4-dihydro-1,4-ethanonaphthalene<sup>15</sup> (5.490 g, 30.46 mmol), hexafluoro-2-butyne (15.2 g, 93.83 mmol, 3.1 equiv), and 30 mL of dichloromethane was stirred at ambient temperature for 15.5 h, in a sealed bottle. The residue was flash-chromatographed (*n*-hexane) to give 7.79 g of 2,3-bis(trifluoromethyl)-1,4,9,10-tetrahydro-9,10-ethenoanthracene (22.8 mmol, 75%). Mp 149.5–150.0 °C (colorless prisms, recrystallized from methanol). Anal. Calcd for  $C_{18}H_{12}F_6$ : C, 63.16; H, 3.53. Found: C, 63.00; H, 3.40.

**(B) 2,3-Bis(trifluoromethyl)-9,10-dihydro-9,10-ethenoanthracene (3e).** A mixture of 2,3-bis(trifluoromethyl)-1,4,9,10-tetrahydro-9,10-ethenoanthracene (obtained as above, 7.79 g, 22.8 mmol) and 2,3-dichloro-5,6-dicyano-1,4-benzoquinone (DDQ) (6.24 g, 27.5 mmol, 1.2 equiv) in 200 mL of benzene was refluxed for 20 h. The solvent was evaporated, and 500 mL of dichloromethane was added and filtered to remove insoluble materials. The organic layer was washed with aqueous 2 N NaOH, brine, and dried over sodium sulfate. Evaporation of the solvent gave 7.38 g of **3e** (21.7 mmol, 95%). Mp 169.0–169.5 °C (colorless cubes, recrystallized from methanol). Anal. Calcd for  $C_{18}H_{10}F_6$ : C, 63.54; H, 2.96. Found: C, 63.31; H, 2.69.

**(C) 2,3-Bis(trifluoromethyl)anthracene.** 2,3-Bis(trifluoromethyl)anthracene was prepared in the similar method as 1,2,3,4-tetrafluoroanthracene with the following modification: <sup>14</sup> 2,3-Bis(trifluoromethyl)-9,10-dihydro-9,10-ethenoanthracene (**3e**) (obtained as above, 4.34 g, 12.8 mmol) and tetraphenyl-1,3-cyclopentadienone (5.40 g, 1.1 equiv) were placed in a 100-mL bottle and sealed. The bottle was heated at 200 °C for 20 h. The residue was flash-chromatographed (*n*-hexane) to give 3.43 g of 2,3-bis(trifluoromethyl)anthracene (86%): mp 138.5–139.0 °C (yellow rodlike plates, recrystallized from *n*-hexane). Anal Calcd for  $C_{16}H_8F_6$ : C, 61.16; H, 2.57. Found: C, 60.94; H, 2.54.

**(D) Dimethyl 2,3-Bis(trifluoromethyl)-9,10-dihydro-9,10-ethenoanthracene-11,12-dicarboxylate (4e).** The 2,3-bis(trifluoromethyl) diester **4e** was prepared by the Diels–Alder cyclization of 2,3-bis(trifluoromethyl)anthracene (3.01

g, 9.59 mmol) and 10.2 g of dimethyl acetylenedicarboxylate (72.4 mmol, 7.5 equiv) in 91% yield (3.96 g, 8.69 mmol). Mp 136.0–136.5 °C (colorless prisms, recrystallized from methanol). Anal. Calcd for  $C_{22}H_{14}O_4F_6$ : C, 57.90; H, 3.09. Found: C, 57.80; H, 3.11.

**(E) 2,3-Bis(trifluoromethyl)-9,10-dihydro-9,10-ethenoanthracene-11,12-dicarboxylic Acid.** Hydrolysis of the above diester **4e** gave the corresponding diacid, 2,3-bis(trifluoromethyl)-9,10-dihydro-9,10-ethenoanthracene-11,12-dicarboxylic acid in 96% yield. IR (KBr,  $cm^{-1}$ ): 3350, O—H; 1700, C=O.

**(F) 2,3-Bis(trifluoromethyl)-9,10-dihydro-9,10-ethenoanthracene-11,12-dicarboxylic Anhydride (1e).** Dehydroxylation of the above diacid gave the anhydride **1e** in 93% yield (method B). IR (KBr,  $cm^{-1}$ ): 1845, 1770, C=O. HRMS ( $M^+$ ) Calcd for  $C_{20}H_8O_3F_6$ : 410.0378. Found: 410.0359.

**Diels–Alder Reactions of the Anhydride 1a–e.** Diels–Alder reactions of the anhydrides **1a–e** were carried out under the similar conditions as unsubstituted **1a**. The adducts were separated as a mixture by flash column chromatography, and the stereoisomers were separated by the specified methods (HPLC, repeated flash column chromatography, and preparative thin layer chromatography). Ratios of the diastereomers were determined from signal integration values in the <sup>1</sup>H NMR spectra.

**Diels–Alder Reaction of 1a with 1,3-Butadiene.** A solution of **1a** (28 mg, 0.10 mmol) in 3 mL of dichloromethane was treated with 1,3-butadiene (460 mg, 8.5 mmol, 85 equiv) at –78 °C (dry ice–acetone), and the reaction vessel was sealed. The mixture was stirred in the sealed bottle at 23 °C for 15 h. Remaining 1,3-butadiene and dichloromethane was removed under reduced pressure. The residue was flash-chromatographed (dichloromethane) to give 33 mg (98%) of the adduct **5a**: mp 222.5–223.0 °C (colorless prisms, recrystallized from ethyl acetate/*n*-hexane). Anal. Calcd for  $C_{22}H_{16}O_3$ : C, 80.47; H, 4.91. Found: C, 80.75; H, 4.93.

**Diels–Alder Reaction of 1b with 1,3-Butadiene.** Two diastereomers were separated by preparative TLC (dichloromethane:*n*-hexane 2:3).

**Anti-adduct (5b):** mp 230.0–231.0 °C (colorless prisms, recrystallized from ethyl acetate/*n*-hexane). Anal. Calcd for  $C_{23}H_{18}O_4 \cdot \frac{1}{5}H_2O$ : C, 76.31; H, 5.12. Found: C, 76.42; H, 4.87.

**Syn-adduct (6b):** mp 233.0–233.5 °C (colorless prisms, recrystallized from ethyl acetate/*n*-hexane). Anal. Calcd for  $C_{23}H_{18}O_4$ : C, 77.08; H, 5.06. Found: C, 77.00; H, 4.99.

**Diels–Alder Reaction of 1c with 1,3-Butadiene.** Two diastereomers were separated by HPLC (15% ethyl acetate/*n*-hexane).

**Anti-adduct (5c):** mp 254.5–255.0 °C (colorless prisms, recrystallized from ethyl acetate/*n*-hexane). Anal. Calcd for  $C_{22}H_{15}NO_5$ : C, 70.77; H, 4.05; N, 3.75. Found: C, 70.90; H, 4.09; N, 3.75.

**Syn-adduct (6c):** mp 194.5–196.0 °C (colorless rods, recrystallized from ethyl acetate/*n*-hexane). Anal. Calcd for  $C_{22}H_{15}NO_5$ : C, 70.77; H, 4.05; N, 3.75. Found: C, 71.05; H, 3.85; N, 4.03.

**Diels–Alder Reaction of 1d with 1,3-Butadiene.** Two diastereomers were separated by flash column chromatography (ethyl acetate:*n*-hexane 1:10).

**Anti-adduct (5d):** mp 272.0–273.0 °C (colorless prisms, recrystallized from ethyl acetate/*n*-hexane). Anal. Calcd for C<sub>22</sub>H<sub>12</sub>O<sub>3</sub>F<sub>4</sub>: C, 66.01; H, 3.02. Found: C, 65.71; H, 2.74.

**Syn-adduct (6d):** mp 242.0–242.5 °C (colorless prisms, recrystallized from ethyl acetate/*n*-hexane). Anal. Calcd for C<sub>22</sub>H<sub>12</sub>O<sub>3</sub>F<sub>4</sub>: C, 66.01; H, 3.02. Found: C, 65.80; H, 2.96.

**Diels–Alder Reaction of 1e with 1,3-Butadiene.** Two diastereomers were separated by flash column chromatography (ethyl acetate:*n*-hexane 1:10).

**Anti-adduct (5e):** mp 290.0 °C (colorless needles, recrystallized from ethyl acetate/*n*-hexane). Anal. Calcd for C<sub>24</sub>H<sub>14</sub>O<sub>3</sub>F<sub>6</sub>: C, 62.08; H, 3.04. Found: C, 61.98; H, 2.98.

**Syn-adduct (6e):** mp 224.0–224.5 °C (colorless prisms, recrystallized from ethyl acetate/*n*-hexane). Anal. Calcd for C<sub>24</sub>H<sub>14</sub>O<sub>3</sub>F<sub>6</sub>: C, 62.08; H, 3.04. Found: C, 62.32; H, 2.83.

**Diels–Alder Reaction of 1a with 2,3-Dimethyl-1,3-butadiene.** A solution of **1a** (28 mg, 0.10 mmol) in 3 mL of dichloromethane was treated with 2,3-dimethyl-1,3-butadiene (34 mg, 0.41 mmol, 4.1 equiv). The mixture was stirred at 23 °C for 15 h, and then 2,3-dimethyl-1,3-butadiene and dichloromethane were removed at reduced pressure. The residue was flash-chromatographed (dichloromethane) to give 36 mg (100%) of **7a**: mp 256.5 °C (colorless prisms, recrystallized from ethyl acetate/*n*-hexane). Anal. Calcd for C<sub>24</sub>H<sub>20</sub>O<sub>3</sub>: C, 80.88; H, 5.66. Found: C, 80.75; H, 5.67.

**Diels–Alder Reaction of 1b with 2,3-Dimethyl-1,3-butadiene.** Two diastereomers were separated by preparative TLC (dichloromethane:*n*-hexane 2:3).

**Anti-adduct (7b):** mp 244.0–245.0 °C (colorless prisms, recrystallized from ethyl acetate/*n*-hexane). Anal. Calcd for C<sub>25</sub>H<sub>22</sub>O<sub>4</sub>: C, 77.70; H, 5.74. Found: C, 77.47; H, 5.51.

**Syn-adduct (8b):** mp 214.0–215.0 °C (colorless flakes, recrystallized from *n*-hexane). HRMS (M<sup>+</sup>) Calcd for C<sub>25</sub>H<sub>22</sub>O<sub>4</sub>: 386.1518, Found: 386.1526.

**Diels–Alder Reaction of 1c with 2,3-Dimethyl-1,3-butadiene.** Two diastereomers were separated by preparative TLC (dichloromethane:*n*-hexane 1:2).

**Anti-adduct (7c):** mp 245.0–248.0 °C (colorless powder, recrystallized from ethyl acetate/*n*-hexane). Anal. Calcd for C<sub>24</sub>H<sub>19</sub>NO<sub>5</sub>: C, 71.81; H, 4.77; N, 3.49. Found: C, 71.65; H, 4.88; N, 3.76.

**Syn-adduct (8c):** mp 243.0–245.0 °C (colorless prisms, recrystallized from ethyl acetate/*n*-hexane). Anal. Calcd for C<sub>24</sub>H<sub>19</sub>NO<sub>5</sub>: C, 71.81; H, 4.77; N, 3.49. Found: C, 71.68; H, 4.66; N, 3.74.

**Diels–Alder Reaction of 1d with 2,3-Dimethyl-1,3-butadiene.** Two diastereomers were separated by flash column chromatography (ethyl acetate:*n*-hexane 1:20).

**Anti-adduct (7d):** mp 267.5–268.0 °C (colorless rods, recrystallized from ethyl acetate/*n*-hexane). HRMS Calcd for C<sub>24</sub>H<sub>16</sub>O<sub>3</sub>F<sub>4</sub>: 428.1036. Found: 428.1064.

**Syn-adduct (8d):** mp 230.5–231.0 °C (colorless prisms, recrystallized from ethyl acetate/*n*-hexane). HRMS Calcd for C<sub>24</sub>H<sub>16</sub>O<sub>3</sub>F<sub>4</sub>: 428.1036. Found: 428.1053.

**Diels–Alder Reaction of 1e with 2,3-Dimethyl-1,3-butadiene.** Two diastereomers were separated by flash column chromatography (ethyl acetate:*n*-hexane 2:25).

**Anti-adduct (7e):** mp 278.5–279.5 °C (colorless prisms, recrystallized from ethyl acetate/*n*-hexane). Anal. Calcd for C<sub>26</sub>H<sub>18</sub>O<sub>3</sub>F<sub>6</sub>: C, 63.42; H, 3.68. Found: C, 63.25; H, 3.31.

**Syn-adduct (8e):** mp 246.0–246.5 °C (colorless prisms, recrystallized from ethyl acetate/*n*-hexane). Anal. Calcd for C<sub>26</sub>H<sub>18</sub>O<sub>3</sub>F<sub>6</sub>: C, 63.42; H, 3.68. Found: C, 63.51; H, 3.59.

**Diels–Alder Reaction of 1a with Cyclopentadiene.** Freshly distilled cyclopentadiene (222 mg, 3.36 mmol, 34 equiv) was added to a solution of **1a** (27 mg, 0.099 mmol) in 3 mL of dichloromethane. The mixture was stirred at 23 °C for 15 h, and then cyclopentadiene and dichloromethane were removed under reduced pressure. The residue was flash-chromatographed (*n*-hexane, followed by dichloromethane) to give 21 mg (63%) of a mixture of the *endo*-adduct **9a** and the *exo*-adduct **10a**, which was separated by flash column chromatography (ethyl acetate:*n*-hexane 1:20).

**Endo-adduct (9a):** mp > 300 °C (colorless prisms, recrystallized from *n*-hexane). Anal. Calcd for C<sub>23</sub>H<sub>16</sub>O<sub>3</sub>: C, 81.16; H, 4.74. Found: C, 81.03; H, 4.61.

**Exo-adduct (10a):** mp 241.0–242.5 °C (colorless rods, recrystallized from ethyl acetate/*n*-hexane). Anal. Calcd for C<sub>23</sub>H<sub>16</sub>O<sub>3</sub>: C, 81.16; H, 4.74. Found: C, 80.95; H, 4.62.

**Diels–Alder Reaction of 1b with Cyclopentadiene.** Four diastereomers were separated by HPLC (10% ethyl acetate/*n*-hexane), and then preparative TLC (dichloromethane:*n*-hexane 2:3).

**Anti-endo-adduct (9b):** mp 265.0–266.0 °C (colorless plates, recrystallized from ethyl acetate/*n*-hexane). Anal. Calcd for C<sub>24</sub>H<sub>18</sub>O<sub>4</sub>: C, 77.82; H, 4.90. Found: C, 77.95; H, 4.73.

**Anti-exo-adduct (10b):** mp 179.5–180.5 °C (colorless prisms, recrystallized from ethyl acetate/*n*-hexane). Anal. Calcd for C<sub>24</sub>H<sub>18</sub>O<sub>4</sub>: C, 77.82; H, 4.90. Found: C, 77.76; H, 4.94.

**Syn-endo-adduct (11b):** mp 244.5–245.5 °C (colorless prisms, recrystallized from ethyl acetate/*n*-hexane). Anal. Calcd for C<sub>24</sub>H<sub>18</sub>O<sub>4</sub>: C, 77.82; H, 4.90. Found: C, 77.65; H, 4.82.

**Syn-exo-adduct (12b):** mp 250.0–250.5 °C (colorless prisms, recrystallized from ethyl acetate/*n*-hexane). Anal. Calcd for C<sub>24</sub>H<sub>18</sub>O<sub>4</sub>: C, 77.82; H, 4.90. Found: C, 77.54; H, 4.85.

**Diels–Alder Reaction of 1c with Cyclopentadiene.** Four diastereomers were separated by HPLC (20% dichloromethane/*n*-hexane).

**Anti-endo-adduct (9c):** mp 296.0–300.0 °C (colorless prisms, recrystallized from ethyl acetate/*n*-hexane). Anal. Calcd for C<sub>23</sub>H<sub>15</sub>NO<sub>5</sub>: C, 71.68; H, 3.92; N, 3.63. Found: C, 71.46; H, 3.85; N, 3.79.

**Anti-exo-adduct (10c):** mp 210.0–211.0 °C (colorless needles, recrystallized from ethyl acetate/*n*-hexane). Anal. Calcd for C<sub>23</sub>H<sub>15</sub>NO<sub>5</sub>: C, 71.68; H, 3.92; N, 3.63. Found: C, 71.85; H, 3.82; N, 3.89.

**Syn-endo-adduct (11c):** mp 279.5–281.5 °C (colorless rods, recrystallized from ethyl acetate/*n*-hexane). Anal. Calcd for C<sub>23</sub>H<sub>15</sub>NO<sub>5</sub>: C, 71.68; H, 3.92; N, 3.63. Found: C, 71.45; H, 3.79; N, 3.90.

**Syn-exo-adduct (12c):** mp 267.0–267.5 °C (colorless prisms, recrystallized from ethyl acetate/*n*-hexane). Anal. Calcd for C<sub>23</sub>H<sub>15</sub>NO<sub>5</sub>·1/2H<sub>2</sub>O: C, 70.05; H, 4.09; N, 3.55. Found: C, 70.24; H, 3.75; N, 3.90.

**Diels–Alder Reaction of 1d with Cyclopentadiene.** Four diastereomers were separated by flash column chromatography (ethyl acetate:*n*-hexane 1:10) and then HPLC (10% chloroform/*n*-hexane for **9d** and **10d**, 2% ethyl acetate/*n*-hexane for **11d** and **12d**).

**Anti-endo-adduct (9d):** mp > 300 °C. HRMS (M<sup>+</sup>) Calcd for C<sub>23</sub>H<sub>12</sub>O<sub>3</sub>F<sub>4</sub>: 412.0723. Found: 412.0716.

**Anti-exo-adduct (10d):** mp 261.5–262.5 °C (colorless rods, recrystallized from *n*-hexane). Anal. Calcd for C<sub>23</sub>H<sub>12</sub>O<sub>3</sub>F<sub>4</sub>: C, 67.00; H, 2.93. Found: C, 66.92; H, 2.72.

**Syn-endo-adduct (11d):** mp 281.5–283.0 °C (colorless rods, recrystallized from *n*-hexane). Anal. Calcd for C<sub>23</sub>H<sub>12</sub>O<sub>3</sub>F<sub>4</sub>: C, 67.00; H, 2.93. Found: C, 66.71; H, 2.71.

**Syn-exo-adduct (12d):** mp 254.5–255.0 °C (colorless rods, recrystallized from *n*-hexane). Anal. Calcd for C<sub>23</sub>H<sub>12</sub>O<sub>3</sub>F<sub>4</sub>: C, 67.00; H, 2.93. Found: C, 67.23; H, 2.94.

**Diels–Alder Reaction of 1e with Cyclopentadiene.** Four diastereomers were separated by HPLC (5% ethyl acetate/*n*-hexane).

**Anti-endo-adduct (9e):** mp 239.5–240.5 °C (colorless rods, recrystallized from ethyl acetate/*n*-hexane). Anal. Calcd for C<sub>25</sub>H<sub>14</sub>O<sub>3</sub>F<sub>6</sub>: C, 63.03; H, 2.96. Found: C, 62.92; H, 2.85.

**Anti-exo-adduct (10e):** mp 238.0–238.5 °C (colorless needles, recrystallized from ethyl acetate/*n*-hexane). Anal. Calcd for C<sub>25</sub>H<sub>14</sub>O<sub>3</sub>F<sub>6</sub>: C, 63.03; H, 2.96. Found: C, 62.83; H, 2.72.

**Syn-endo-adduct (11e):** mp > 300 °C (colorless prisms, recrystallized from ethyl acetate/*n*-hexane). Anal. Calcd for C<sub>25</sub>H<sub>14</sub>O<sub>3</sub>F<sub>6</sub>: C, 63.03; H, 2.96. Found: C, 62.75; H, 2.66.

**Syn-exo-adduct (12e):** mp > 300 °C (colorless prisms, recrystallized from ethyl acetate/*n*-hexane). Anal. Calcd for C<sub>25</sub>H<sub>14</sub>O<sub>3</sub>F<sub>6</sub>: C, 63.03; H, 2.96. Found: C, 62.81; H, 2.74.

**Diels–Alder Reaction of 1a with 1,3-Cyclohexadiene.**

A mixture of **1a** (74 mg, 0.27 mmol) and 1,3-cyclohexadiene (2.64 g, 33 mmol, 122 equiv) was heated in a sealed bottle at 100 °C for 15 h, and then the volatile was evaporated and the residue was flash-chromatographed (dichloromethane:*n*-hexane 1:1) to give 55 mg of a mixture of the products (**13a** and **14a**), which was separated by HPLC (ethyl acetate 5%/*n*-hexane).

**Endo-adduct (13a):** mp > 300 °C (colorless rods, recrystallized from ethyl acetate/*n*-hexane). Anal. Calcd for C<sub>24</sub>H<sub>18</sub>O<sub>3</sub>·<sup>1</sup>/<sub>2</sub>H<sub>2</sub>O: C, 79.32; H, 5.27. Found: C, 79.15; H, 5.01.

**Exo-adduct (14a):** mp 267.0–268.5 °C (colorless prisms, recrystallized from ethyl acetate/*n*-hexane). Anal. Calcd for C<sub>24</sub>H<sub>18</sub>O<sub>3</sub>: C, 81.34; H, 5.12. Found: C, 81.05; H, 5.04.

**Diels–Alder Reaction of 1b with 1,3-Cyclohexadiene.**

Four diastereomers were separated by HPLC (7% ethyl acetate/*n*-hexane and then 15% dichloromethane/*n*-hexane).

**Anti-endo-adduct (13b):** mp 220.0–222.0 °C. HRMS (M<sup>+</sup>) Calcd for C<sub>25</sub>H<sub>20</sub>O<sub>4</sub>: 384.1362, Found: 384.1315.

**Anti-exo-adduct (14b):** mp 216.0–218.0 °C (colorless needles, recrystallized from ethyl acetate/*n*-hexane). Anal. Calcd for C<sub>25</sub>H<sub>20</sub>O<sub>4</sub>: C, 78.11; H, 5.24. Found: C, 77.83; H, 5.24.

**Syn-endo-adduct (15b):** mp 280.5–281.0 °C. HRMS (M<sup>+</sup>) Calcd for C<sub>25</sub>H<sub>20</sub>O<sub>4</sub>: 384.1362. Found: 384.1355.

**Syn-exo-adduct (16b):** mp 266.5–268.5 °C (colorless powder, recrystallized from ethyl acetate/*n*-hexane). Anal. Calcd for C<sub>25</sub>H<sub>20</sub>O<sub>4</sub>: C, 78.11; H, 5.24. Found: C, 77.90; H, 5.40.

**Diels–Alder Reaction of 1c with 1,3-Cyclohexadiene.**

Four diastereomers were separated by HPLC (10% ethyl acetate/*n*-hexane and then 25% chloroform/*n*-hexane).

**Anti-endo-adduct (13c):** mp > 300 °C. HRMS (M<sup>+</sup>) Calcd for C<sub>24</sub>H<sub>17</sub>NO<sub>5</sub>: 399.1107. Found: 399.1138.

**Anti-exo-adduct (14c):** mp 294.0–295.0 °C (colorless needles, recrystallized from ethyl acetate/*n*-hexane). Anal. Calcd for C<sub>24</sub>H<sub>17</sub>NO<sub>5</sub>: C, 72.17; H, 4.29; N, 3.51. Found: C, 72.04; H, 4.19; N, 3.70.

**Syn-endo-adduct (15c):** mp > 300 °C. HRMS (M<sup>+</sup>) Calcd for C<sub>24</sub>H<sub>17</sub>NO<sub>5</sub>: 399.1107. Found: 399.1135.

**Syn-exo-adduct (16c):** mp 276.0–277.5 °C (colorless rods, recrystallized from ethyl acetate/*n*-hexane). Anal. Calcd for C<sub>24</sub>H<sub>17</sub>NO<sub>5</sub>: C, 72.17; H, 4.29; N, 3.51. Found: C, 72.37; H, 4.36; N, 3.76.

**Diels–Alder Reaction of 1d with 1,3-Cyclohexadiene.**

Four diastereomers were separated by HPLC (5% ethyl acetate/*n*-hexane).

**Anti-endo-adduct (13d):** mp > 300 °C (colorless needles, recrystallized from *n*-hexane). HRMS (M<sup>+</sup>) Calcd for C<sub>24</sub>H<sub>14</sub>O<sub>3</sub>F<sub>4</sub>: 426.0879. Found: 426.0873.

**Anti-exo-adduct (14d):** mp > 300 °C (colorless rods, recrystallized from ethyl acetate/*n*-hexane). Anal. Calcd for C<sub>24</sub>H<sub>14</sub>O<sub>3</sub>F<sub>4</sub>: C, 67.61; H, 3.31. Found: C, 67.67; H, 3.05.

**Anti-endo-adduct (15d):** mp > 300 °C (colorless needles, recrystallized from *n*-hexane). HRMS (M<sup>+</sup>) Calcd for C<sub>24</sub>H<sub>14</sub>O<sub>3</sub>F<sub>4</sub>: 426.0879. Found: 426.0866.

**Anti-exo-adduct (16d):** mp 288.5–289.5 °C (colorless rods, recrystallized from ethyl acetate/*n*-hexane). Anal. Calcd for C<sub>24</sub>H<sub>14</sub>O<sub>3</sub>F<sub>4</sub>: C, 67.61; H, 3.31. Found: C, 67.63; H, 3.01.

**Diels–Alder Reaction of 1e with 1,3-Cyclohexadiene.**

Four diastereomers were separated by HPLC (10% ethyl acetate/*n*-hexane).

**Anti-endo-adduct (13e):** mp 263.0–264.0 °C (colorless prisms, recrystallized from *n*-hexane). HRMS (M<sup>+</sup>) Calcd for C<sub>26</sub>H<sub>16</sub>O<sub>3</sub>F<sub>6</sub>: 490.1004. Found: 490.1013.

**Anti-exo-adduct (14e):** mp 242.0–242.5 °C (colorless needles, recrystallized from *n*-hexane). Anal. Calcd for C<sub>26</sub>H<sub>16</sub>O<sub>3</sub>F<sub>6</sub>: C, 63.68; H, 3.29. Found: C, 63.50; H, 3.16.

**Syn-endo-adduct (15e):** mp > 300 °C (colorless prisms, recrystallized from ethyl acetate/*n*-hexane). HRMS (M<sup>+</sup>) Calcd for C<sub>26</sub>H<sub>16</sub>O<sub>3</sub>F<sub>6</sub>: 490.1004. Found: 490.0998.

**Syn-exo-adduct (16e):** mp > 300 °C (colorless rods, recrystallized from ethyl acetate/*n*-hexane). HRMS (M<sup>+</sup>) Calcd for C<sub>26</sub>H<sub>16</sub>O<sub>3</sub>F<sub>6</sub>: 490.1004. Found: 490.1009.

**Measurements of Relative Rates of the Diels–Alder Reactions with 2,3-Dimethyl-1,3-butadiene.**

A mixture of **1a** (4.1–5.9 mg, 0.015–0.022 mmol) and a substituted anhydride (**1x**, one of the anhydrides **x** = **b–e**, 0.014–0.022 mmol) was dissolved in 0.5 mL of CD<sub>2</sub>Cl<sub>2</sub> in an NMR tube. To this solution was added 3.4–4.9 mg (0.041–0.060 mmol) of 2,3-dimethyl-1,3-butadiene at ambient temperature. The sample tube was well shaken and loaded into the spectrometer, and all the measurements were conducted at 23 °C. After 30 min from the addition of 2,3-dimethyl-1,3-butadiene, signal accumulation was started (96 s duration for accumulation, and 1704 s interval of accumulation). Signal integration values of the starting materials (**1a** and **1x**) and the products (**5a**, **5x**, and **6x**) were obtained in each measurement, and the logarithms of [(**1x** + **5x** + **6x**)/**1x**] (=Y) and [(**1a** + **5a**)/**1a**] (=X) were calculated. Plot of ln Y against ln X gave a straight line with regression more than 0.999, and the slope of the line provides the relative value of the second-order rate constants (*k<sub>x</sub>*/*k<sub>H</sub>*). Then the *k<sub>x</sub>*/*k<sub>H</sub>* is distributed into the values of *anti*- and *syn*-side of the dienophile in proportion to the *anti*/*syn* product ratio.

**Supporting Information Available:** <sup>1</sup>H NMR assignments, the calculated transition state energies (total energies and relative energies), orbital pictures (and energies) of the LUMO and lowest few unoccupied orbitals of the dienophile **1a–e** and experimental results in toluene (32 pages). This material is contained in libraries on microfiche, immediately follows this article in the microfilm version of the journal, and can be ordered from the ACS; see any current masthead page for ordering information.

JO9520811